

University of Mississippi

eGrove

---

Electronic Theses and Dissertations

Graduate School

---

1-1-2021

# GRAPHENE SAND COMPOSITES AND THEIR APPLICATIONS IN WATER TREATMENT

Abdulla Nusair

*University of Mississippi*

Follow this and additional works at: <https://egrove.olemiss.edu/etd>

---

## Recommended Citation

Nusair, Abdulla, "GRAPHENE SAND COMPOSITES AND THEIR APPLICATIONS IN WATER TREATMENT" (2021). *Electronic Theses and Dissertations*. 2167.

<https://egrove.olemiss.edu/etd/2167>

This Thesis is brought to you for free and open access by the Graduate School at eGrove. It has been accepted for inclusion in Electronic Theses and Dissertations by an authorized administrator of eGrove. For more information, please contact [egrove@olemiss.edu](mailto:egrove@olemiss.edu).

# **GRAPHENE SAND COMPOSITES AND THEIR APPLICATIONS IN WATER TREATMENT**

A Thesis Presented for the Degree of  
Master of Science in Engineering Science with an Emphasis in Civil Engineering

The University of Mississippi

Abdulla Nusair  
December 2021

Copyright January 2022 by Abdulla Nusair

All Rights Reserved

## Abstract:

Water scarcity and the emergence of new contaminants are making the world in need of renewable water resources. Slow sand filtration is looked at as an affordable and easy method to filter water with a few weaknesses such as clogging and the inability to remove complex matrix ingredients. To overcompensate these limited weaknesses, graphene-coated sand was studied. Ottawa, concrete, and masonry sand were used, using a reduction method to transform a coating of sugar into elemental carbon in N<sub>2</sub> atmosphere at temperatures reaching 750°C. After that, the synthesized materials were activated using sulfuric acid. To verify the effectiveness of the coating process used, a digital microscope, Raman spectroscopy, scanning electron microscope, and energy-dispersive X-ray spectroscopy were implemented. After that, flow-through columns were used to evaluate the ability of the different materials to remove turbidity and bacteria. Due to the additional expense related to the activation process, columns packed with graphene sands were tested alongside the non-activated ones as well as columns containing the raw sands.

The digital microscope revealed that rounded (Ottawa sand) particles were coated less efficiently than sub-angular and angular particles (concrete, and masonry sand). The Raman spectroscopy revealed the formation of G and D bands in all graphitized sands suggesting complete graphitization of the sugar and the presence of defect site necessary for the adsorption of contaminants. Furthermore, the peak intensity was 30% higher in concrete and masonry graphitized sands compared to Ottawa graphitized sand solidifying the visual characterization.

SEM on the samples revealed the formation of carbon sheets 10 nm thick and EDS results backed up the geological identification of the sands with quantification of the elements.

The graphene-coated sand dominated the turbidity stress test. The graphene-coated Ottawa (GCOS) sand lasted high turbidity by more than 15% longer when compared to raw Ottawa sand (ROS). And the effluent turbidity value was 25% lower in GCOS compared to ROS.

Bacteria removal in both Ottawa and masonry sand increased with graphene coating, concrete sand maintained removal higher than 90% when coated. The difference in effectiveness of the activation is minuscule and cannot be justified with the current work.

## *Dedication*

*This work is completely dedicated to my respectful and loving family who have been motivating me throughout this journey. My grandfather the engineer Abdulla Al-Rabaie was the reason I peruse the field of engineering. My parents Jafar, and Abeer who offered me endless love and support that I can never repay. My older sister Sara has always been my mentor in life and the person I look up to the most. Last but most definitely not least my younger brother Mahmoud who has been my life companion and the spark of joy whenever I needed it the most.*

## Abbreviations:

### Acronym:

AC	Activated Carbon
AGCCS	Activated Graphene Coated Concrete Sand
AGCMS	Activated Graphene Coated Masonry Sand
AGCOS	Activated Graphene Coated Ottawa Sand
ASTM	American Society for Testing and Materials
CCL	Contaminant Candidate List
CEC	Contaminants of Emerging Concerns
COD	Chemical Oxygen Demand
$d_e$	Effective Diameter
DOC	Dissolved Organic Carbon
EC	Electrical Conductivity
EDS	Energy Dispersive X-Ray Spectroscopy
EPA	Environmental Protection Agency
GCCS	Graphene Coated Concrete Sand
GCMS	Graphene Coated Masonry Sand
GCOS	Graphene Coated Ottawa Sand
HLR	Hydraulic Loading Rate
NEERI	National Environmental Engineering Research Institute
OM	Organic Matter
RCS	Raw Concrete Sand
RMS	Raw Masonry Sand
ROS	Raw Ottawa Sand
SEM	Scanning Electron Microscope
SSF	Slow Sand Filtration
TOC	Total Organic Carbon
TSS	Total Suspended Solids
UASB	Up-flow Anaerobic Sludge Blanket
UNESCO	United Nations Educational, Scientific and Cultural Organization
WWAP	World Water Assessment Program
WWTP	Waste Water Treatment Plants

## Units:

°C	Degree celsius
°C/min	Degree Celsius per minute
cm	Centimeter
g	Grams
hr	hour
km	Kilometer
KV	kilovolts
lbs	Pounds
m	Meter
m/h	Meter per hour
mg/l	Milligram per liter
min	Minute
ml	Milliliter
ml/min	Milliliter per minute
mm	Millimeter
MPN/100 ml	Most probable number per 100 milliliters
μS/cm	MicroSiemens per centimeter
ng/l	Nanogram per liter
nm	Nanometer
NTU	Nephelometric turbidity unit



## Acknowledgments

Throughout the writing of this thesis, a great deal of support and assistance was received by many...

First and foremost, I would like to thank my advisors, Professor Hunain Alkhateb and Dr. Matteo D'Alessio, whose great expertise guided me throughout the research. And to whom I owe this achievement. The constant mentoring helped me increase my knowledge both in the academic and practical fields to a higher level.

I would like to acknowledge the civil engineering faculty members, whose valuable and insightful guidance helped me improve upon my work. Particularly, Professor Ahmed Al-Ostaz and professor Cristiane Surbeck for being members of my thesis committee. Mrs. Grace Rushing provided very useful resources, workspaces, materials, and equipment critical to the completion of this research.

I would also like to thank collaborators from the University of Mississippi, Mr. Paul Matthew Lowe from the mechanical engineering department, for his valuable support with the technical measures during the building of the set-up. Dr. Vijayasankar Raman from the department of pharmacy, for his help with the training and use of the scanning electron microscope. And our collaborators from Jackson State University, professor Paresh Chandra Ray from the department of chemistry, physics, and atmospheric sciences, for providing us with his expertise and equipment during the characterization process.

Additionally, I want to show my gratitude towards my senior graduate colleagues, Rami Alsughayer, Hussam Al-Zubi, and Abdel Rahman Awawdeh, For their academic advice, great help during the characterization process, water collection for filtration, and great emotional support. Not forgetting my undergraduate assistant, Cheyenne Ethridge, whose great help in the lab was a huge factor in achieving this work in a shorter period of time.

Last but not least, special thanks to B&B Concrete Co, and Lafayette Ready Mix Company, for their very generous donation of 300 lbs. of sand used for this experiment.

## Keywords:

Low-cost water and wastewater treatment;

Slow Sand Filtration; Graphene-Coated Sand;

Raman Spectroscopy;

Scanning Electron Microscopy (SEM);

Energy Dispersive X-Ray;

Spectroscopy (EDS);

Water Quality;

Turbidity.

# Contents

CHAPTER 1. INTRODUCTION.....	1
1.1. Background .....	1
1.1.1. Water Resources, Water, and Wastewater Treatment .....	1
1.1.2. History and Development of Water and Wastewater Treatment.....	1
1.1.3. The Emergence of New Contaminants.....	2
1.1.4. Sand Filtration in Water and Wastewater Treatment .....	3
1.1.5. Weaknesses of SSFs.....	7
1.1.6. Carbon Based Materials in Water Treatment .....	8
1.1.7. Graphene in Water Treatment .....	9
1.2. Research objectives .....	10
1.3. Thesis layout.....	10
CHAPTER 2. SAND SUGAR COATING AND GRAPHITIZATION.....	11
2.1. Raw Materials.....	11
2.1.1. The Sand.....	11
2.1.2. Sugar.....	13
2.2. Production Methodology .....	13
2.2.1. Sand Dry Sieving.....	13
2.2.2. Sand Wet Sieving .....	15
2.2.3. Sand Sugar Coating .....	16
2.2.4. Graphitization of the Sugar-Coated Sands .....	16
2.2.5. Activation of the Graphene Coated Sands.....	18
CHAPTER 3. GRAPHENE COATED SAND CHARACTERIZATION .....	19
3.1. Visual Characterization .....	19
3.1.1. Equipment and Methodology .....	19
3.1.2. Results .....	19
3.2. Raman Spectroscopy .....	20
3.2.1. Equipment and Methodology .....	21
3.2.2. Results .....	21

3.3. Scanning Electron Microscope.....	23
3.3.1. Equipment and Methodology .....	23
3.3.2. Results .....	24
3.4. Energy Dispersive X-Ray Spectroscopy (EDS) .....	28
3.4.1. Equipment and Methodology .....	29
3.4.2. Results .....	29
CHAPTER 4. WATER FILTRATION APPLICATIONS .....	31
4.1. Water Source Selection .....	31
4.2. Setups' Materials and Preparation.....	32
4.2.1. Water Quality Setup .....	32
4.2.2. Turbidity Stress Test Setup .....	35
4.3. Analytical methods.....	36
4.3.1. Turbidity .....	36
4.3.2. Electrical Conductivity (EC) .....	37
4.3.3. Total coliforms and <i>E. coli</i> .....	37
4.4. Results and discussions .....	38
4.4.1. Total Coliform and <i>E. coli</i> Removal .....	38
4.4.2. Turbidity Stress Test.....	40
4.4.3. EC:.....	42
CHAPTER 5. CONCLUSIONS: .....	44
FUTURE RESEARCH: .....	46
Bibliography.....	47
Appendices .....	59

## List of Tables:

Table 1.1: Design criteria for SSFs. ....	4
Table 1.2: Efficiencies of removal of different parameter in sand filters. ....	7
Table 2.1: Properties and composition of the acquired sand. ....	13
Table 2.2: Particle size characterization used for SSF. ....	15
Table 3.1: EDS analysis results for raw sand. ....	29
Table 3.2: EDS analysis results for graphene coated and activated graphene coated sand. ....	30
Table 4.1: Water Quality tests on water bodies in Oxford, MS. ....	31

## List of Figures:

Figure 3.1: Microscope pictures (X150) and coating efficiencies of the prepared composites GCOS, GCCS, and GCMS. [GCOS: Graphene coated Ottawa san., GCCS: Graphene coated concrete sand; GCMS: Graphene coated masonry sand] ..... 20

Figure 3.2: Raman spectra of the prepared composites GCOS, GCCS, and GCMS. [GCOS: Graphene coated Ottawa san., GCCS: Graphene coated concrete sand; GCMS: Graphene coated masonry sand]. ..... 22

Figure 3.3: SEM images of raw sands ROS (A&C), RCS (B), and RMS (D). [ROS: raw Ottawa sand; RCS: raw concrete sand; RMS: raw masonry sand] ..... 24

Figure 3.4: SEM images of GCOS (A&B), GCCS (C), and GCMS (D). [GCOS: Graphene coated Ottawa san., GCCS: Graphene coated concrete sand; GCMS: Graphene coated masonry sand]..... 26

Figure 3.5: SEM image of GCMS. [GCMS: graphene coated masonry sand]..... 27

Figure 3.6: SEM images of AGCOS (A&B), AGCCS (C), and AGCMS (D). [AGCOS: activated graphene coated Ottawa san.; AGCCS: activated graphene coated concrete sand; AGCMS: activated graphene coated masonry sand]..... 28

Figure 4.1 Schematic of the eleven-column setup used for water quality tests. .... 33

Figure 4.2: Representation of the dimensions and layers heights of the columns used in the water quality test..... 34

Figure 4.3: Representation of the dimensions and layers heights of the columns used in the turbidity stress test. .... 36

Figure 4.4: Total Bacteria Removal for ROS, RCS, RMS, GCOS, GCCS, GCMS, AGCOS, AGCCS, and AGCMS filtration columns [ROS: raw Ottawa sand; RCS: raw concrete sand; RMS: raw masonry sand; GCOS: Graphene coated Ottawa sand, GCCS: Graphene coated concrete sand; GCMS: Graphene coated masonry sand; AGCOS: activated graphene coated Ottawa sand; AGCCS: activated graphene coated concrete sand; AGCMS: activated graphene coated masonry sand]. ..... 39

Figure 4.5: Turbidity removal and influent turbidity during the turbidity stress test for GCOS. [GCOS: Graphene coated Ottawa sand]..... 41

Figure 4.6: Turbidity removal and influent turbidity during the turbidity stress test for ROS. [ROS: raw Ottawa sand]..... 42

Figure 4.7: electrical conductivity for ROS, RCS, RMS, GCCS, GCMS, AGCOS, AGCCS, AGCMS, O, C, and M. [ROS: raw Ottawa san., GCCS: raw concrete sand; GCMS: raw masonry sand; GCOS: graphene coated Ottawa san., GCCS: graphene coated concrete sand; GCMS: graphene coated masonry sand; AGCOS: activated graphene coated Ottawa san.,

AGCCS: activated graphene coated concrete sand; AGCMS: activated graphene coated masonry sand].....	43
Figure A.1: Raw sand preparation.....	60
Figure A.2: Sand sugar coating and graphitization. ....	60
Figure A.3:Water source (lake Patsy) and water collection. ....	61
Figure A.4: the eleven-column setup.....	62
Figure A.5:Activation process using sulfuric acid. ....	62

# CHAPTER 1. INTRODUCTION

## 1.1. Background

### 1.1.1. Water Resources, Water, and Wastewater Treatment

The overpopulation in the last decade has caused an increase in the production of wastewater. According to UNESCO, about 1500 km<sup>3</sup> of wastewater is produced annually worldwide, which is equivalent to approximately six times the amount of river water in the world (UNESCO, 2003). This overpopulation leads to a prediction of even higher water consumption in the coming decades with a large demand especially in agriculture which is responsible for 70% of the global water abstraction (UNESCO, 2015). Research has shown that the urbanization level variations are consistent with the variations on the integrated pollution index (Chamara & Koichi, 2017; Wang et al., 2008). Approximately 65% of the current world population lives in areas that experience water scarcity. Additionally, 6.5% of people live in areas where water consumption is twice as much of the locally available renewable water resources (UNESCO, 2017). Depletion of water resources is shifting the world to seek affordable alternative resources. With advancements in wastewater management, wastewater is being viewed more as a reliable water resource that reuses, recycles, and recovers the otherwise treated and disposed of costly expense (Dev et al., 2021).

### 1.1.2. History and Development of Water and Wastewater Treatment

Throughout history, water treatment techniques have been implemented to purify water before drinking. In the ancient Sanskrit medical writings (2000 BC), a primitive method of



water purification was done by boiling water before passing it through sand and gravel (Mays, 2013) which is still being used in the modern world with a few enhancements. Furthermore, wastewater treatment techniques have been developed as means necessary for saving water and reusing wastewater as a new water resource (Tchobanoglous et al., 2004). Wastewater management dates back to as early as 2500 BCE in the Indus Valley Civilization (Lofrano & Brown, 2010). Modern-day wastewater treatment plants (WWTPs) consist of a multitude of stations that start with wastewater in all forms and end with an effluent that is safe to be discharged back into the environment. Each of the WWTPs' stations has a specific function; these stations are selected during the design process depending on the type of influent being treated. Sand filtration is widely used in WWTPs in the tertiary treatment stage (Tyagi et al., 2009; Andreadakis & Christoulas, 1982), due to the need for increased removal of suspended solids and organic matter to provide more efficient disinfection (Mackenzie Leo Davis, 2020).

### 1.1.3. The Emergence of New Contaminants

Due to the discharge of wastewater effluent back into the environment, any contaminants that remain untreated are introduced to the aquatic ecosystem, which has a major effect on aquatic species (Wakelin et al., 2008) and reflects on human health (Mangalgi et al., 2015). While the effluent discharged has been monitored for legacy contaminants and trace metals by the US EPA (US EPA, 2015a), many of the untreated contaminants of emerging concerns (CECs) are still on the drinking water contaminant candidate list (CCL) (US EPA, 2014) being released without being subject to EPA drinking water regulations (Nawaz & Sengupta, 2019). Stimulants, antibiotics, beta-blockers, and steroids are some of the most commonly detected CECs in treated and untreated wastewaters (Viegas et al., 2020; Weigel et al., 2004). Long-term exposure to low concentrations (ng/L) of these compounds causes aquatic

toxicity and cellular death (Antunes et al., 2013). In humans, they alter gene expressions that cause gastrointestinal and renal effects (Wojcieszynska & Guzik, 2020).

#### 1.1.4. Sand Filtration in Water and Wastewater Treatment

Layers of sand and gravel are used as porous media for the water to pass through and undergo three methods of purification: physical straining of suspended particles (filtration), chemical sorption, and assimilation a process where nutrients are broken down by aerobic microbes that occurs at the upper layer (*Schmutzdecke* or biolayer) of the filters (Verma et al., 2017). The biological breakdown process represents the leading removal mechanism followed by adsorption, mechanical filtration, and degradation (Adin, 2003). The biolayer forming at the top 0-2 cm of sand consists mainly of algae and bacteria that deplete the natural organic matter (OM) present in the influent that is synthesized by algae (Tyagi et al., 2009). It helps retain pathogens and contains bacteria that aid in the process of biological removal of nitrates (Aslan & Cakici, 2007). About a third of OM synthesized by algae passes into the filter bed where it is utilized by the bacteria (Tyagi et al., 2009). Over time, in the lower portion of the filter, biomass build-up occurs, inhabits anoxic processes (Campos et al., 2002), and further enhances its removal performances. Sand filters are affordable to manufacture, maintain, and run. They are effective in removing suspended colloids and pathogens from water (Mackenzie Leo Davis, 2020). They are also able to remove taste and smells making a large improvement to the drinking water in a water filtration system. This makes them a perfect candidate for water and wastewater treatment.

Among the three most common sand filters, rapid sand filters, upward flow sand filter, and slow sand filters (SSF) implemented so far, SSF represents the most effective and most commonly used for treating drinking water, wastewater, and rainwater due to the lack of chemical aids or skilled labor required (Visscher, 1990; L Huisman & Wood, 1974). SSFs have been also used in rural communities, developing countries, and in the aftermath of natural disasters. Table 1.1 summarizes basic design criteria for SSFs.

*Table 1.1: Design criteria for SSFs.*

<b>Design criterion</b>	<i>Recommended level</i>	<i>References</i>
<i>Design period</i>	10 – 15 years	
<i>Filtration rate</i>	0.1 – 0.2 m <sup>3</sup> /m <sup>2</sup> /h	Visscher, 1990
<i>Minimum filter bed height</i>	0.5 – 0.6 m	
	Typical SSF size (0.15-0.3)	Visscher, 1990
<i>Type of filter media (effective size in mm)</i>	Natural sand (0.43)	Tyagi et al., 2009
	Quartz sand (0.71-1.25)	Slavik et al., 2013
	Silica sand (1-2)	Zheng et al., 2010
<i>Uniformity coefficient</i>	Preferably below 3	Visscher, 1990
<i>Average construction cost per 1000 m<sup>3</sup>/day unit</i>	US \$42,000	Visscher, 1990

The design period of SSF ranges between 10 to 15 years, which increases its economic value because a short design period reduces the stress of expensive perpetual design on developing countries, and that reduces eroding the limited available resources (Visscher, 1990). In addition, the cost of construction varies with the size of the build and its capacity. For example, according to a report from the national environmental engineering research institute (NEERI), SSF was 10 – 20 % cheaper in construction costs than conventional filters (Sundaresan & Paramasivam, 1982). SSFs are easy to operate and maintain, as suspended solids and colloidal matter are collected on the top layer of the filter, unskilled workmen with basic tools or a simple portable conveyor belt (L Huisman & Wood, 1974).

The packing material, fine granular inert material, with an effective size between 0.15-0.3 mm acts as an additional effective filtration media (Visscher, 1990). Among the granular inert materials available, sand has been widely used due to its availability and low cost. Sand can be purchased at a very low cost (Young-Rojanschi & Madramootoo, 2014; Dubey et al., 2015; Kumar et al., 2020) or is locally available (Gupta et al., 2012; Rahman & Praseetha, 2016; Achazhiyath Edathil et al., 2019). Based on the type(s) of sand used, SSF filters can either be monolithic (e.g., Elbana et al., 2012) or can contain multiple layers in succession ranging from finer (top) to coarser (bottom) sand (Bourne et al., 2006). In the presence of a multilayer configuration, the flow rate is governed by the permeability of the top finer layer.

The hydraulic loading rate (HLR), defined as the ratio between the flow rate and the area of the filter, is inversely proportional to the contact time between the feed water and the filter media and consequently to the efficiency of the SSF. Researches have used HLR ranging

between 0.0083 m/h and 0.38 m/h (Nakhla & Farooq, 2003; Bourne et al., 2006; Tyagi et al., 2009; Katukiza et al., 2014) with lower HLR showing higher efficiency. For example, Tyagi et al., (2009) observed higher filtration capacity in the presence of low (0.14 m/h) HLR than in presence of moderate to high (0.19 to 0.24 m/h) HLR. Moreover, Katukiza et al., (2014) reported increased chemical oxygen demand (COD) removal (by 6%), total organic carbon (TOC), and dissolved organic carbon (DOC) removal (by 5%) in the presence of small HLR (0.0083 m/h vs. 0.0163 m/h). Due to the increased thickness of the biolayer and the occurrence of clogging within the packing material, HLR decreases with the age of the filtration unit. Mature filters experience reduced HLR. However, cleaning activities (e.g., scraping/removing the biolayer and or backwashing the filtration unit) can increase the HLR.

The effective diameter of the particles ( $d_{10}$  or  $d_e$ ) can also significantly impact the performance of the SSF. The effective diameter ( $d_e$ ) is known as the screen opening that allows 10% of the total mass of the sand sample to pass through. As  $d_e$  decreases the efficiency increases, especially in terms of total suspended solids (TSS) removal (Ives, 1980).

The removal efficiency of an SSF unit is significantly impacted by the quality of the feed water used. Table 1.2 summarizes some of the removal efficiencies obtained in terms of COD, turbidity, and TSS using different influents, media, and HLRs.

Table 1.2: Efficiencies of removal of different parameter in sand filters.

SOURCE OF WATER	PARAMETERS REMOVAL (%)				References
	<i>COD</i>	<i>BOD</i>	<i>Turbidity</i>	<i>SS</i>	
Unchlorinated WWTP effluent	33-40 <sup>A</sup>	76-83 <sup>A</sup>	33-62	50-71 <sup>A</sup>	(Nakhla & Farooq, 2003)
	12-35 <sup>B</sup>	33-65 <sup>B</sup>		22-43 <sup>B</sup>	
Greywater	90 <sup>C</sup>	61-67		65	(Katukiza et al., 2014)
	84 <sup>D</sup>				
UASB* reactor effluent	77	85	92	89	(Tyagi et al., 2009)

<sup>A</sup> Fine sand media

<sup>B</sup> coarse sand media

<sup>C</sup> Low HLR

<sup>D</sup> High HLR

\* Up-flow anaerobic sludge blanket.

### 1.1.5. Weaknesses of SSFs

SSFs are limited by a few weaknesses. The clogging of SSFs is a phenomenon caused by the buildup of fine particles inside the filtration media. This buildup causes head loss and reduces the flow rate or stops the process completely (Rodgers et al., 2004). The issue of clogging can be mitigated by regular cleaning of the filters. Either by removing the top layer or backwashing. SSFs are limited in adsorption by the surface area of the sand particles used. The existence of complex matrix ingredients in the influent blocks the limited surface area of the sand, which limits the efficiency of SSFs in organic and micropollutants removal (Kumar et al., 2020). This limitation cannot be tackled without making changes to the surface morphology of the sand.

### 1.1.6. Carbon Based Materials in Water Treatment

Carbon had been widely used in water treatment. One of the most commonly used carbon derivatives is activated carbon (AC) (Gupta et al., 2012). AC had been studied as an adsorbent of emerging contaminants extensively. Marques et al. (2017) studied the adsorption to two PhCs (Paracetamol and Clofibric acid). Using a two-step air thermal oxidation process, Polyacrylonitrile (PAN) heavy tow textile fibers were carbonized under a flow of argon as an inert gas then activated using CO<sub>2</sub> to create Activated Carbon Cloth (ACC), along with powdered carbon and granular carbon. The results showed 50% removal of the paracetamol and 80% removal of the clofibric acid in the solution. Because activated carbon is expensive other work looked into cheaper alternative production methods. Most organic materials are rich in carbon, anything from wood, agricultural by-products like fruit stones and seeds hulls can be used to synthesize ACs. In (Viegas et al., 2020) research a carob waste-derived powdered activated carbon was assessed in the removal of diclofenac and sulfamethoxazole. (Leite et al., 2017) synthesized AC from avocado seeds. Torrellas et al. (2015) Prepared AC using peach stones as the carbon source, and H<sub>3</sub>PO<sub>4</sub> for chemical activation to adsorb caffeine, diclofenac (anti-inflammatory drug), and carbamazepine (psychiatric drug). Because of the hydrophobicity of the AC produced the sorption of carbamazepine was the highest at a Q<sub>max</sub> value of 335 mg/g. In another study (Torrellas et al., 2016) compared the previously synthesized peach stone AC, and an AC made from rice husks with a similar method, against commercial carbon to adsorb ibuprofen. Where it was observed that rice husk AC was superior. The problem with AC is that after it is used for adsorption it is difficult to regenerate for reuse, and even after regeneration it is not as efficient as newly synthesized AC.

### 1.1.7. Graphene in Water Treatment

Graphene is one of the newest additions to the carbon family. First discovered in 2004 by the two physicists Kostya Novoselov, and Andre Geim (Geim & Novoselov, 2007) graphene had been renowned as one of the most versatile materials to be discovered. Graphene is a single 2-dimensional sheet of carbon atoms arranged in a hexagonal lattice. It's proven as the ideal nanocomposite in many materials (Fan et al., 2017). The approach of creating graphene around sand as a coating layer to improve its applications in water treatment emerged in the last decay (Gupta et al., 2012; Dubey et al., 2015). Gupta et al (2012) studied the graphitization of the sugar at different temperatures, proving that the best dehydration reaction of the sure occurs at 750 °C. The possibility of using this composite in water purification was also studied as an adsorbent, showing the superiority of graphene to AC as an adsorbent (Gupta et al., 2012). Dubey et al (2015) found 93% removal of chromium oxide is possible from using the graphene sand composite. Other more recent research looked into the use of graphene sand composites as adsorbents (Moradi & Azizian, 2016; Rahman & Praseetha, 2016; Achazhiyath Edathil et al., 2019). Just like AC, it has been proven that graphene sand composite could also be synthesized from affordable organic materials such as sugar-rich brewery effluent (Kumar et al., 2020) and arenga palm sugar (Zularisam et al., 2017). Kumar et al (2020) used the synthesized graphene sand composite as a filtration media of sand filters, to compare its efficiency water treatment against raw sand, and the manganese dioxide graphene coated sand. The results showed that even graphene sand made from affordable sugar sources outperformed raw sand in metal removal, biological degradation, and breakthrough time.



## 1.2. Research objectives

The main objectives of this thesis are; 1) assessing the use of different types of sand in synthesizing graphene coated sand from the dehydrogenation of sugar in an inert environment under high temperatures. 2) The different characteristics of the sands (particle size, and shape; quartz content) are studied to have a better understanding of their effects on the coating efficiency and quality. 3) Characterizing the graphene coated sand to understand the composition of the synthesized material. 4) Investigating the effects of activation with sulfuric acid on the graphene coated sand. 5) Studying the effect, of the graphene coating and the activated graphene coating offer to the quality of the sand as a filtration media. 6) Comparing the synthesized materials with the raw materials in various water quality tests (turbidity removal, electrical conductivity, and total coliform and *E. coli* removal).

## 1.3. Thesis layout

This thesis is divided into five chapters. Chapter 1 gives a brief introduction about water issues, SSF in water treatment, and the use of carbon-based materials in water treatment. Chapter 2 gives an idea about the materials and the methodology used during this study. Chapter 3 discusses the characterization methods and results of the synthesized materials. Chapter 4 explains the methodology of using the synthesized material in water filtration and the water quality tests used during the study. Lastly, Chapter 5 summarizes the conclusions of this study.

## CHAPTER 2. SAND SUGAR COATING AND GRAPHITIZATION

### 2.1. Raw Materials

Graphene sand consisted of two major components. The nucleus of the formation of the graphene coating was the sand, and the layer of graphene was created from the graphitized sugar around the sand particle.

#### 2.1.1. The Sand

Silica Density Sand ASTM-D1556 (HUMBOLDT Mfg. Co., Elgin, Illinois), Concrete Mix Sand ASTM-C33 (Lafayette Ready-Mix, Oxford, MS), and Masonry Sand (Lafayette Ready-Mix, Oxford, MS) were used as the nuclei of the three graphene coated sands used throughout the study.

##### 2.1.1.1. Silica Density Sand *ASTM-D1556* (Ottawa Sand)

The Ottawa sand is mined from Ottawa, Illinois. It is used for ASTM tests due to its naturally rounded shape and its high content of pure quartz. 90% of the particles are well rounded or rounded, and only 10% of the particles are subangular to angular. It has a quartz content greater than 95% and lithic fragments less than 5%. It contains very few particles that pass the No.200 sieve (fine content, 75 $\mu$ m opening size) or retain on the No.10 sieve (2.0mm opening size). The coefficient of uniformity of less than 2. Ottawa sand has a white clear color.

#### 2.1.1.2. Concrete Sand *ASTM-C33*

This type of sand meets the ASTM guidelines to be used in concrete. Geologically it is classified as being coarse to medium with crushed gravel. It consists of approximately 85% quartz, and 15% rock fragments with a particle shape distribution of 60% sub-angular, 35% sub-rounded, and 5% rounded particles. For grain size particles between 0.25 (Sieve No. 40) and 0.85 mm (Sieve No. 60), approximately 37% and 32% of the mass of the sand was retained on sieves No. 40 and 60 and the coefficient of uniformity was 2.3. Due to its high content of crushed rock fragments this sand had a light brown color.

#### 2.1.1.3. Masonry Sand

Usually known as finer concrete sand, this type of sand is used for mason work. It is classified as coarse to very coarse sand, with a quartz content of about 99% with a 1% rock fragment. The particle shape is a mixture of sub-rounded and sub-angular particles. After running the sieve analysis, it was observed that around 14.4% and 60.5% of the mass of the sand was retained on sieves No. 40 and 60 respectively, and the coefficient of uniformity is 1.8. Similar to the Ottawa sand, the masonry sand has a white clear color. Table 2.1 summarizes the geological properties of the sands used during the study.

Table 2.1: Properties and composition of the acquired sand.

	Ottawa Sand	Concrete Sand	Masonry Sand:
<i>Geological Description</i>	fine/medium sand	Coarse/medium sand with gravel	Coarse/very coarse sand
<i>Composition</i>	>95% Quartz, <5% Lithic fragments	85% Quartz, 15% Rock fragments	99% Quartz, 1% Rock fragments
<i>Particles Shape</i>	90% well rounded/rounded, 10% subangular/angular	60% sub-angular, 35% sub-rounded, 5% rounded	A mixture of sub-rounded and sub-angular particles

### 2.1.2. Sugar

Two sources of sugar, *Great Value* cane sugar (Walmart) and Reagents Sucrose (Cole-Parmer, Vernon Hills, Illinois) were used. The cane sugar was used in the preliminary testing stage during the planning phase of the mass production methodology. All final products used were made with pure sucrose.

## 2.2. Production Methodology

A four-step approach was developed to prepare the different graphene sands used throughout the study. The acquired raw materials required processing before coating, due to containing a mixture of particle sizes unfit for slow sand filtration.

### 2.2.1. Sand Dry Sieving

The sieving process varied between the different types of sand. USA Standard Sieves (HUMBOLDT Mfg. Co. Elgin, Illinois) were used. The sieves range from a No.4 with a 4.75

mm opening to a sieve No.200 with a 0.075 mm opening. The desired size for sand filtration is between 0.25 to 0.85 mm hence the material retained on sieves No.40 and 60 were used for this study. Visscher (1990) suggested the use of sand particles ranging between 0.15 and 0.3 mm (Visscher, 1990). The actual size of the particles were measured using a microscope to obtain the actual particle sizes to ensure they fall within the desired particle.

#### 2.2.1.1. Ottawa Sand Dry Sieving

Ottawa sand was sifted manually through a No.20 sieve to remove unwanted large particles. No further dry sieving was done as the smallest particles that pass sieve No.50 were already removed as part of the manufacturing process before retail to meet the ASTM-D1556 standard. Particle size distribution and other basic properties are available in Table 2.2.

#### 2.2.1.2. Concrete and Masonry Sand Dry Sieving

Concrete and Masonry sands first had a broad distribution of sizes. Initially, the sand was manually sifted through a No.20 (0.85 mm). After that, to prevent overloading of smaller sieves, 200 g of the passing sand was placed in a No.40 sieve over a No.60 (multiple No.40 and 60 sieves were used at once to expedite the process). The full stack of sieves was placed in a shaker for 15 min at a time and the retained material was stored. The concrete sand yielded the least amount of material making it the type of sand that requires the most effort. Particle size distribution and other basic properties are available in Table 2.2.

Table 2.2: Particle size characterization used for SSF.

<i>Particle size</i>	<i>Sand</i>		
	<i>Ottawa Sand</i>	<i>Concrete</i>	<i>Masonry Sand</i>
<i>Desired particle size for SSF</i>	between 0.15 - 0.3 mm <sup>[1]</sup>		
<i>Size range after sieving</i>	between 0.25 - 0.85 mm		
<i>% of particles retained on Sieves</i>	99%	69.30%	74.90%
<i>Actual particle size (mm)</i>	0.169 - 0.493	0.171 - 0.316	0.138 - 0.260
<i>Actual particle size (Avg)</i>	0.330 mm	0.243 mm	0.194 mm

<sup>[1]</sup> Visscher, 1990

### 2.2.2. Sand Wet Sieving

Even after the dry sieving some fine particles and clay remain between the desired sand particles. Due to the inefficiency of dry sieving to remove the excess finer particles from the larger particles, wet sieving was also implemented. Dry sieved sand was placed in a No.40 sieve over a No.60 sieve and washed continuously while stirring in the sieves until clean water was observed. After that, the sand was washed multiple times with distilled water to remove any soluble minerals from the tap water. In the end, the washed sand was placed in an oven to dry overnight at 90°C to ensure that it was completely dry before weighing it for the addition of the sugar in the coating process. Part of the Sand prepared from this step was used for the raw material columns named raw Ottawa sand (ROS), raw concrete sand (RCS), and raw masonry sand (RMS). The other part of the sand was further processed to produce the graphene coated sands.

### 2.2.3. Sand Sugar Coating

The coating process started by weighing 200 g of the sand with 20 g of sugar, for a total addition of sugar equivalent to 10% of the sands' weight (Kumar et al., 2020) in a 1000 ml beaker with distilled water. The mixture was stirred and heated at 90 °C until completely dry. In the presence of concrete and masonry sands, some of the produced material was partially agglomerated. The material was sifted through a No.20 sieve and the passing material, representing the well-coated sand, was separated from the retained agglomerated particles. This process was only studied during a preliminary stage involving small batches and it was discarded during the mass production stage due to its limited to no effect on the final product. The mass production process was relatively long due to the large amounts of sand needed. To enhance the mass production process, 600 g of sand were placed in the beaker with 60 g of sugar, and a hand blender was used at a low setting to keep the mixture homogenous. To ensure that the sugar-coated sand was preserved as dry as possible, it was directly stored in an oven well below the softening point of sugar crystals, 60 °C, until the full batch was ready to go into the furnace for the graphitization process.

### 2.2.4. Graphitization of the Sugar-Coated Sands

For the sugar coating to turn into graphene the combustion reaction of the sugar should be eliminated in the graphitization chamber and the extraction of oxygen was required for the graphitization to occur. A combustion reaction in sugar occurs when high temperature is applied and transforms it into carbon dioxide and water. However, in the absence of oxygen and with enough heat, the reaction changes from combustion to dehydrogenation and transforms sugar into graphenic carbon and water as shown in the following equations:

*Sugar combustion (Equation 1):*



*Sugar dehydrogenation (Equation 2):*



Clay planting pots were used as crucibles for the mass production of the graphene coated sand, as they withstand temperatures up to 1300°C and heated in N<sub>2</sub> atmosphere, in an atmosphere-controlled muffle furnace (Across International, NJ, USA). The chamber was first depressurized using a vacuum pump then pumped with Nitrogen gas, this flushing of the system was repeated two times to reduce the amount of trace oxygen left due to an imperfect vacuum. The furnace temperature was programmed following the heating pattern applied by Gupta et al. (2012) as follows:

1. Starting from room temperature to 100°C at a rate of 2.5°C/min in 30 min and held for 30 min.
2. The temperature was ramped to 200°C at a rate of 3.3°C/min in 30 min and held for 60 min, to ensure all the sugar is melted (the sugar melting point is around 186°C) and formally coating the sand particles.
3. Additional ramp to 450°C was followed at a rate of 4.1°C/min in 2 hr and held for 2 hr.
4. A final ramp to 750°C at a rate of 5°C/min in 2 hr and held for 3 hr, to ensure complete graphitization of the sugar.

The resulting material made from the three types of sand were named graphene coated Ottawa Sand (GCOS), graphene coated concrete sand (GCCS), and graphene coated masonry sand (GCMS). These sands were then washed in buckets with flowing water from underneath to clean out any fine carbon material caused by imperfect coating as these might cause clogging



in the filters later on. Then the washed graphene coated sands were dried in an oven at 90 °C until completely dry. In total 6 kg of each material was produced. Half of the quantity was stored and the other half was further processed with activation.

### 2.2.5. Activation of the Graphene Coated Sands

Activation of carbon produces a larger number of adsorption sites (Dubey et al., 2015). Currently available suggested the activation of the carbon coated sand using sulfuric acid (Gupta et al., 2012; Dubey et al., 2015; Rahman & Praseetha, 2016). During this study, the more conservative method (Kumar et al., 2020) was followed and the graphene-coated sands were placed in beakers containing 0.5 M sulfuric acid with a ratio of 2 ml for every gram of graphene-coated sand. The beakers were left undisturbed for 30 min, before being washed with distilled water until neutral pH, and later dried in an oven overnight at 90 °C until completely dry. The resulting materials (after activation with sulfuric acid) were named activated graphene-coated Ottawa sand (AGCOS), activated graphene-coated concrete sand (AGCCS), and activated graphene-coated masonry sand (AGCMS). The activation process significantly impacts the overall cost of the filtration unit due to the cost of the activation chemicals (e.g., sulfuric acid). Therefore, the activated graphene-coated sands were tested against the non-activated graphene-coated sands to evaluate the economic feasibility of this additional step.

## CHAPTER 3. GRAPHENE COATED SAND CHARACTERIZATION

### 3.1. Visual Characterization

The washed graphene coated sands were studied visually using a digital microscope. This characterization method was developed to find the differences in the coating efficiencies among the different types of sand.

#### 3.1.1. Equipment and Methodology

For this test, the well-coated to not well-coated particles ratio was calculated using a Keyence VHX-600 digital microscope with a 150X zoom lens. A representative sample of approximately 30 grains of each type of sand was placed under the lens. Completely or mostly coated particles were counted as coated while poorly or not coated particles were counted as non-coated.

#### 3.1.2. Results

Among the three types of sand used, GCCS had the best coating efficiency (well-coated grains: approximately 88%), followed by GCMS (well-coated grains: approximately 75%) and GCOS (well-coated grains: approximately 47%). According to these results, the quartz content had a limited impact on the coating efficiency. In fact, the sand with the lowest quartz content (concrete sand, 85%), and the sand with the highest quartz content (masonry sand, 99%), performed better than Ottawa sand (quartz content: 95%) (Figure 3.1). In contrast with the

quartz content, the shape of the particle significantly impacts the coating efficiency. Angular particles yield better results than rounded particles (Figure 3.1).


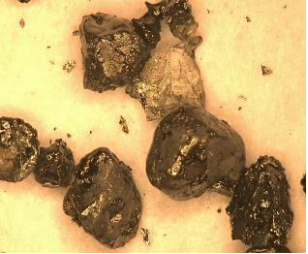

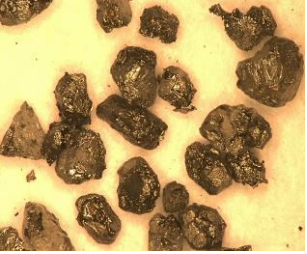
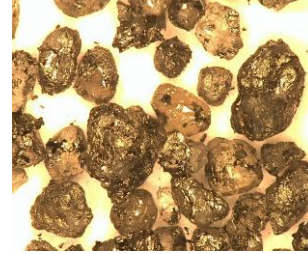
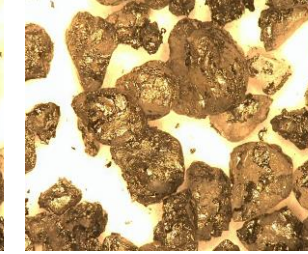
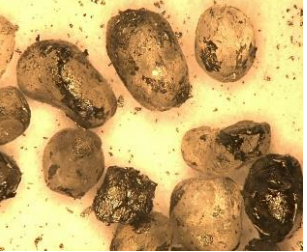
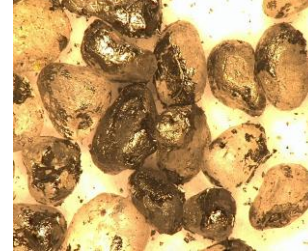

	1	2	3	% of Coated Particles
GCCS				88%
GCMS				75%
GCOS				47%

Figure 3.1: Microscope pictures (X150) and coating efficiencies of the prepared composites GCOS, GCCS, and GCMS. [GCOS: Graphene coated Ottawa sand., GCCS: Graphene coated concrete sand; GCMS: Graphene coated masonry sand]

### 3.2. Raman Spectroscopy

Raman Spectroscopy is an analytical method that works by detecting Raman scattered light. This kind of scattering was first observed in 1928 by the Indian physicist C.V. Raman (Raman & Krishnan 1928). When light hits a molecule the majority of the light is scattered with the same energy as the energy of the projected light (Larkin, 2011). On very rare occasions (approximately 1 in 10 million photons) the light is inelastically scattered in what is known as

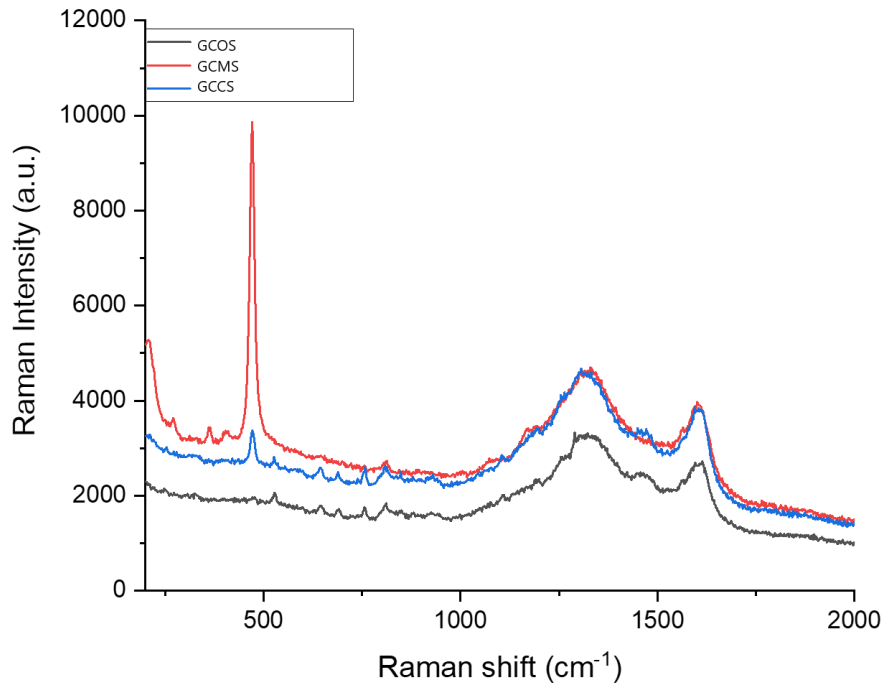
Raman scattering where the energy between molecules is transferred to the scattered photons (Ewen Smith & Dent, 2019). Each material has a unique Raman shift. Studying the variation in the Raman shifts helps characterize materials (Larkin, 2011).

### 3.2.1. Equipment and Methodology

For this work, a MacroRAM Raman spectrometer (Haribo Scientific) with a 785 nm diode-pumped solid-state laser as the light source was used. To minimize possible interferences, a solid-state material holder was used. The solid-state holder is made of carbon-plated steel therefore a silicon wafer was needed to stop the light source from coming in contact with the sample holder. A nonionic surfactant known as Triton X-100 was used to glue the wafer onto the sample holder. Triton X-100's high viscosity helped hold the silicon wafer on the sample holder at an upright position. Furthermore, Triton X-100 was also used to glue the sand samples onto the silicon wafer. The silicon wafer's Raman Shift had to be measured first by itself to be later subtracted from the results as this device is a macro Raman spectrometer and it gives results for a larger area than micro Raman spectrometers that might include the background.

### 3.2.2. Results

Figure 3.2 highlights the results of the Raman spectroscopy on the three types of sand (GCOS, GCCS, and GCMS).



*Figure 3.2: Raman spectra of the prepared composites GCOS, GCCS, and GCMS. [GCOS: Graphene coated Ottawa sand., GCCS: Graphene coated concrete sand; GCMS: Graphene coated masonry sand].*

The Raman spectra results showed the evolution of D and G bands as a result of the carbonization of the sugar. The increase in peak intensity in GCCS and GCMS adhere with the previous data in the visual characterization, the 30% increase in the peak intensity in GCCS and GCMS when compared to GCOS suggests that the formation of graphenic material is higher with angular particle shape than rounded. The formation of the D band around  $1300\text{ cm}^{-1}$  suggests the presence of a defect site in the material which equates to higher absorption. The formation of sharp G bands around  $1600\text{ cm}^{-1}$  suggests complete graphitization of the material (Gupta et al., 2012 ; Rahman & Praseetha, 2016)

### 3.3. Scanning Electron Microscope

SEM is a microscope that utilizes a focused beam of high-energy electrons to generate high-resolution images of the samples' morphology (Rahman & Praseetha, 2016). This method of microscopy was used for the first time by the German electrical engineer Max Knoll in 1935 (McMullan, 2006). The high resolution is mainly generated due to the use of X-Ray as the light source. X-Ray has a wavelength between 0.01-10 nm, which allows the SEM to have a resolution between 1-20 nm. Optical microscopes are the limited wavelength of optical light (White light wavelength, 400-700 nm), which limits the resolution to 200-250 nm (McMullan, 2006).

#### 3.3.1. Equipment and Methodology

The SEM was done on all nine samples of sand used in the filtration (ROS, RCS, RMS, GCOS, GCCS, GCMS, AGCOS, AGCCS, AGCMS). First, the samples needed to be coated with a thin layer of platinum. This thin conductive layer inhibits charging (a phenomenon that gives rise to anomalous-contrast in SEM images in observing a non-conductive specimen), reduces thermal damage, and improves the topographic examination of the samples (Watt, 1978). The samples were secured on aluminum stubs using double-sided carbon stickers. After the application of the tape on the stubs, a small spatula was used to sprinkle a few particles on the sticky surface. A dry air spray can was used to remove any excess material. All nine stubs were hosted inside a sputter coating chamber (Desk V Denton Vacuum) that depressurizes to  $5 \times 10^{-4}$  Torr and uses a DC current (30 mA) to eject platinum atoms and deposit them onto the surface of the samples, this was done for 150 sec. The thickness of the coating layer was 0.11

Å, measured using a film deposition monitor (INICON SQM-160). The stubs were then placed in a sample holder. The Sample holder was placed inside the microscopy chamber. A JSM-7200f scanning electron microscope (JEOL Ltd.) with a Schottky field emission as the electron source was used. All images were taken at a working distance of 10 mm and 10 kV voltage.

### 3.3.2. Results

The topography of the raw sand is shown in figure 3.3 [A) ROS, B) RCS, C) ROS at higher magnification ( $\times 300$ ), and D) RMS.]

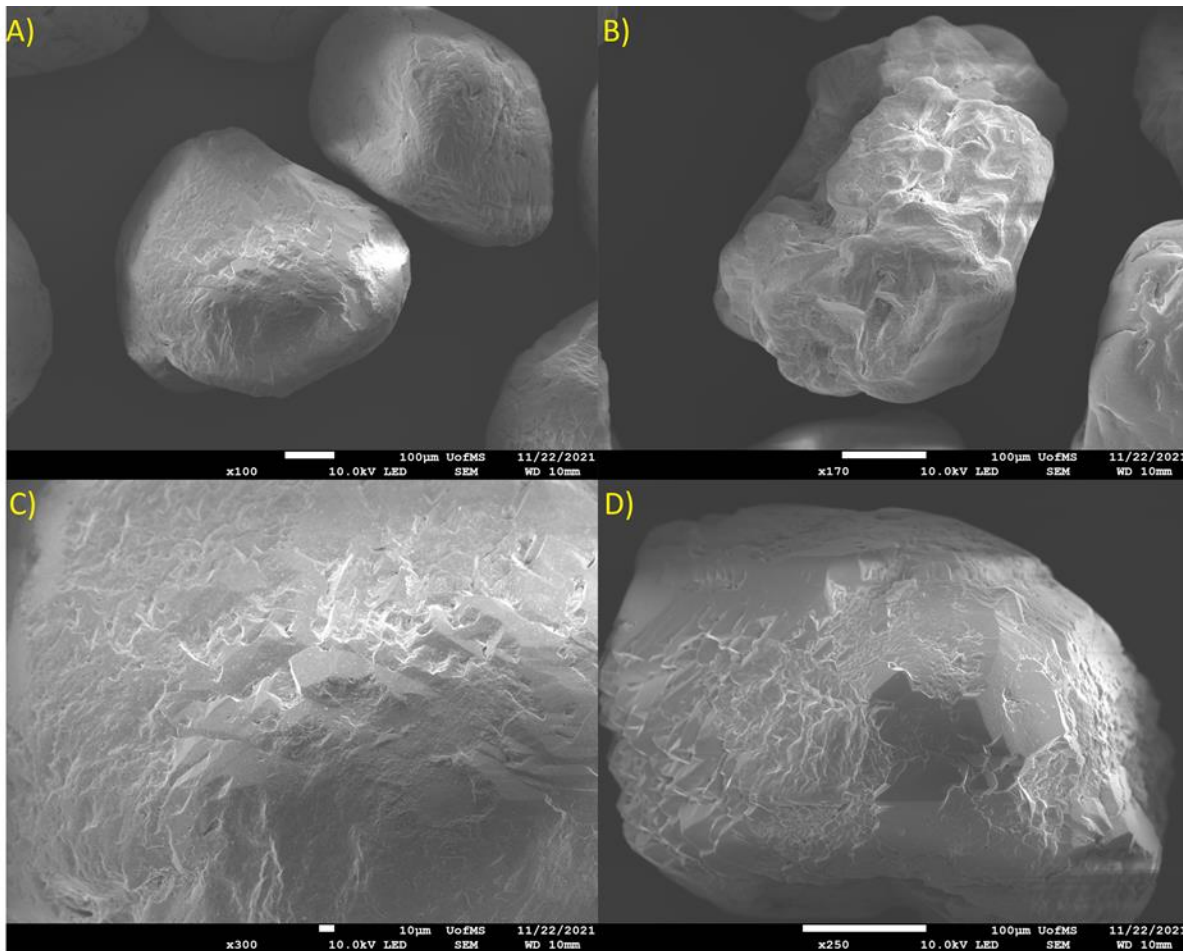


Figure 3.3: SEM images of raw sands ROS (A&C), RCS (B), and RMS (D). [ROS: raw Ottawa sand; RCS: raw concrete sand; RMS: raw masonry sand]

The results solidify the results from the digital microscopy. Additionally, the topography of the sand particle surface can be seen. The surface of RCS is rougher compared to the surface of ROS and RMS. This roughness could be the factor that attributes to the higher efficiency of graphene coating on RCS. RMS surface is slightly rougher than ROS. ROS surface appears to be smooth even at high magnification ( $\times 300$ ).

Figure 3.4 shows the graphene coated sand before activation [A&B) GCOS at different magnifications, C) GCCS, D) GCMS]. The morphology of the coating layer suggests the formation of a graphene-like material. The outward protruding thin sheets of carbon are visible on all three types of sand. The surface of the sheets formed on GCOS were flat and parallel to the surface with fewer protrusions than GCCS and GCMS. The surface morphology of the graphene formed on GCCS and GCMS has more wrinkles and follows the rugged surface of the sand particles.



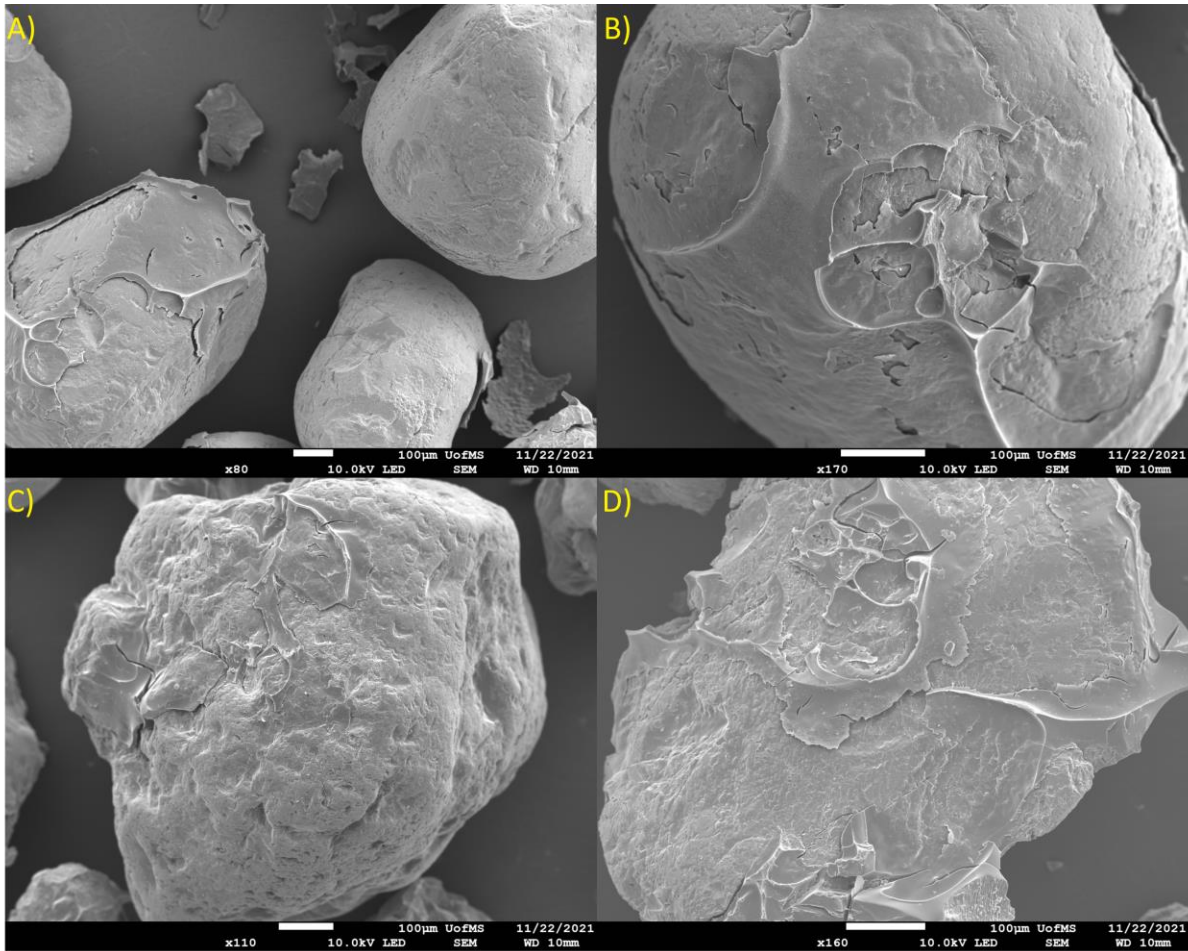
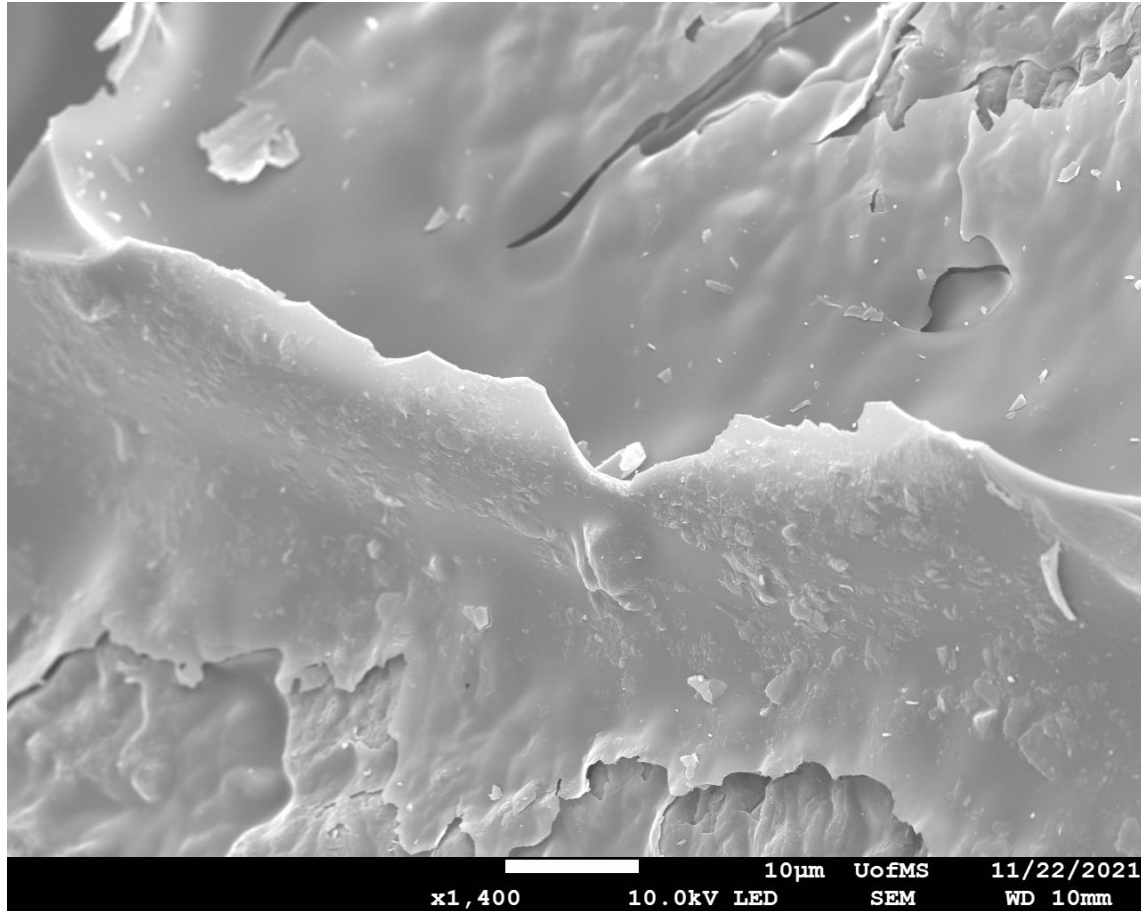


Figure 3.4: SEM images of GCOS (A&B), GCCS (C), and GCMS (D). [GCOS: Graphene coated Ottawa sand, GCCS: Graphene coated concrete sand; GCMS: Graphene coated masonry sand]

The thin sheets of carbon formed on the surface can be seen more clearly in figure 3.5 of GCMS. The layer thickness was measured. Values measured ranged from 10 to 100 nm.



*Figure 3.5: SEM image of GCMS. [GCMS: graphene coated masonry sand]*

Finally, for the activated graphene coated sand (figure 3.6) [A&B) AGCOS, C) AGCCS, D) AGCMS]. The same protrusions are still present with more cracking on the surface of the carbon sheets.

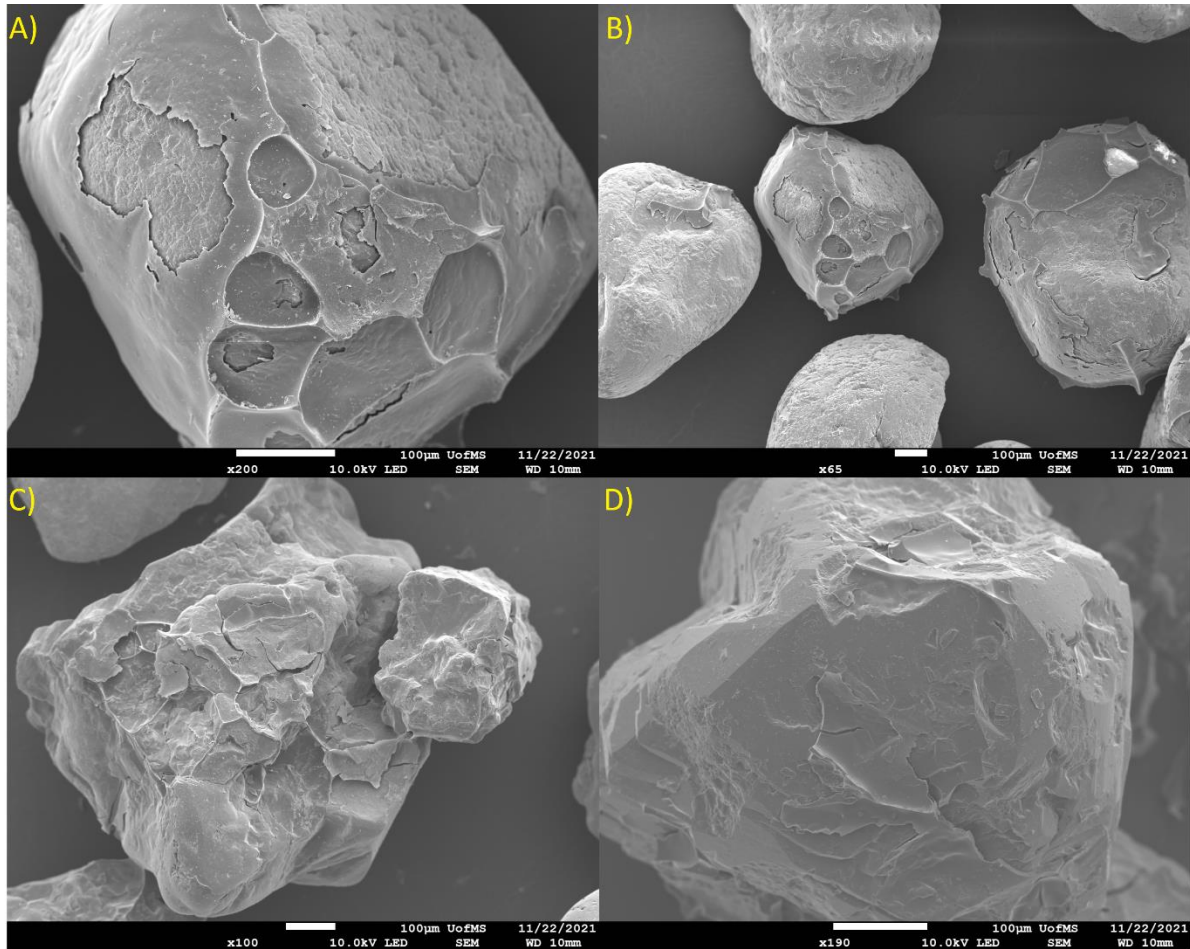


Figure 3.6: SEM images of AGCOS (A&B), AGCCS (C), and AGCMS (D). [AGCOS: activated graphene coated Ottawa sand; AGCCS: activated graphene coated concrete sand; AGCMS: activated graphene coated masonry sand]

### 3.4. Energy Dispersive X-Ray Spectroscopy (EDS)

EDS is an analytical method used to identify the elemental composition of the material. The science behind it is very similar to that of Raman spectroscopy, with the exception that electron beams are used to excite the molecule and displace the electrons from their orbits. This displacement releases radiation energy. The radiation energy emitted from each element is distinctive in its energy level and proportional counts correlates to the quantity of the element.

### 3.4.1. Equipment and Methodology

The device used to measure the X-Ray dispersion was an X-Max 80 (Oxford Instruments) already attached to the SEM. The detector size is 80 mm, and the voltage used was between 0 to 10 KV. The same samples were studied during the SEM with no further modification. Two approaches were taken while studying the elemental compositions of the samples. For the raw sand, an average was taken for ten particles to further study the silica content of the sands. As for the coated and activated sand, multiple particles of up to twelve particles were studied and only the best coated (highest carbon content) was taken into consideration to further solidify the efficiency of coating on the particles.

### 3.4.2. Results

Although the elemental analysis for the raw sand (Table 3.1) complied with the consecutive silica (quartz) content of each type of sand, the presence of carbon was also abundantly available in the materials. this can only mean that the sand has organic materials, which could be ingredients of remains of seashells most commonly present in beach sands. RMS still remains the purest followed by ROS. RCS has the lowest silica content and the highest amount of extra metals (aluminum, iron, and nickel).

*Table 3.1: EDS analysis results for raw sand.*

<b>Sample\Element</b>	<b>Weight (%) by average</b>						
	<i>Si</i>	<i>O</i>	<i>C</i>	<i>Al</i>	<i>Fe</i>	<i>Br</i>	<i>Ni</i>
<i>ROS</i>	39.45	43.35	16.24	0.8	0	0.17	0
<i>RCS</i>	33.47	46.28	15.83	2.28	1.76	0	0.37
<i>RMS</i>	40.35	43.41	16.19	0.07	0	0	0

The elemental analysis of the carbon coated and activated carbon coated sands (Table 3.2) matches with previous data. The carbon content was found to be highest in GCCS and AGCCS. Carbon content was lowest in GCOS and AGCOS denoting the low coating efficiency of the Ottawa sand. Sulfur was present in all three activated sand showing a slight change in the composition post-activation with the sulfuric acid.

*Table 3.2: EDS analysis results for graphene coated and activated graphene coated sand.*

<i>Sample\Element</i>	<b>Weight (%)</b>						
	<i>Si</i>	<i>O</i>	<i>C</i>	<i>Al</i>	<i>Fe</i>	<i>Ni</i>	<i>S</i>
<i>GCOS</i>	17.34	25.38	56.04	0.18	0.38	0.64	0
<i>GCCS</i>	8.1	19.9	70.8	0.5	0	0.7	0
<i>GCMS</i>	17.7	18.3	63.6	0.5	0	0	0
<i>AGCOS</i>	20	28.7	50.3	0.5	0	0	0.5
<i>AGCCS</i>	8	19.4	68.8	2.6	0	0	1.1
<i>AGCMS</i>	13	30.9	54.9	0.3	0	0	0.8

## CHAPTER 4. WATER FILTRATION APPLICATIONS

Two experimental setups were implemented to test the different packing materials under 1) extremely high level of turbidity observed after heavy rain events if surface waters are used as feed water or in the aftermath of natural disasters, and 2) normal conditions. The turbidity stress test was conducted using a smaller setup consisting of two columns packed with ROS and GCOS, while the rest of the water quality tests were performed using eleven columns packed with ROS, RCS, RMS, GCCS, GCMS, AGCOS, AGCCS, and AGCMS.

### 4.1. Water Source Selection

After investigating all nearby options in Oxford Mississippi (Table 4.1), lake Patsy was selected due to its higher bacteria content. Lake Patsy (acreage: 7.6) is a lake located within Lamar park and it is opened to the public for fishing, mainly containing bream and catfish (<https://www.mdwfp.com/fishing-boating/community-assistance/lake-patsy/>). Water was collected twice per week using multiple 5-gal buckets off the fishing deck closer to the center of the lake. As for the turbidity stress test, tap water spiked with high turbidity was used.

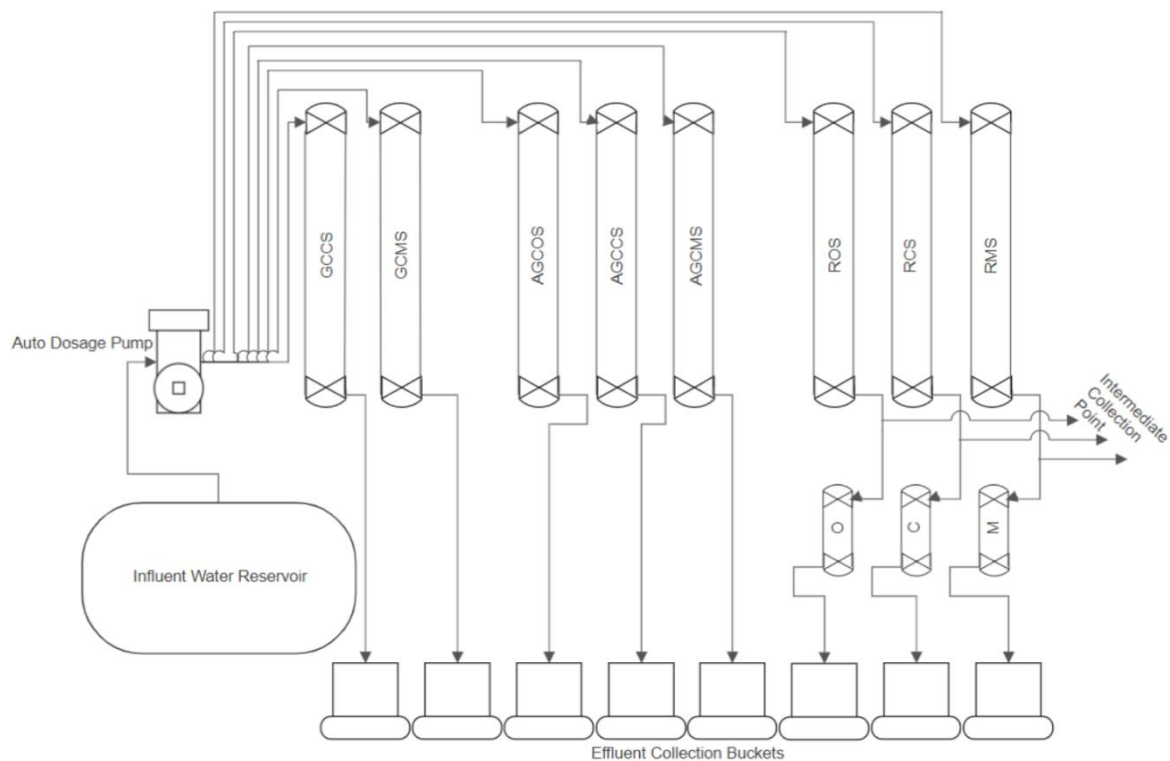
Table 4.1: Water Quality tests on water bodies in Oxford, MS.

<b>Water bodies</b>	<b>pH</b>	<b>NO<sub>3</sub></b>	<b>NO<sub>2</sub></b>	<b>Total Hardness</b>	<b>Total Alkalinity</b>	<b>Total Coliform</b>	<b>Electrical Conductivity</b>
				<i>mg/L</i>		<i>MPN/100 ml</i>	<i>μS/cm</i>
<i>Silver pond</i>	6.9	-	-	30	45	620	210
<i>Sardis lake</i>	6.9	-	-	40	50	2282	10
<i>Patsy lake</i>	6.8	-	-	25	40	1607	30
<i>Lexington pond</i>	6.9	-	-	30	40	1607	210

## 4.2. Setups' Materials and Preparation

### 4.2.1. Water Quality Setup

The water quality setup consisted of a 30 gal water tank that held the lake water used during the test as the influent. Eight tubings (Masterflex L/S 14, inner diameter: 1.6 mm) were passed from the reservoir through 4 Masterflex Easy-Load II double pump heads in parallel into each of the eight columns. The pump heads were connected to a Masterflex L/S precision console drive. A Masterflex three-way stopcock fitting was used before and after each of the columns in case to control the flow and ease of collection from these points. Five of the eight columns were running as one-stage filtration columns (GCCS, GCMS, AGCOS, AGCCS, AGCMS). Meanwhile, three of the eight columns were running as two-stage filtration columns (ROS, RCS, and RMS) and were coupled in series with smaller columns filled with AGCOS, AGCCS, and AGCMS respectively. The smaller columns filled with AGCOS, AGCCS, and AGCMS as the filtration media were named O, C, and M respectively for easier differentiation during the data interpretation. Similarly, three-way stopcocks were used before and after the three small columns. The effluent from all eight running lines poured into 5 gal buckets. Figure 4.1 shows the full schematic of the water quality eleven columns setup and the tubing line connections.



*Figure 4.1 Schematic of the eleven-column setup used for water quality tests.*

All columns were made from polyvinyl chloride (PVC) pipes (Home Depot). The eight larger pipes were 62 cm tall with an inner diameter of 52 mm. The three smaller tubes were 13 cm tall with an inner diameter of 38 mm (Figure 4.2). All pipes were closed at both ends with adequate PVC rounded fittings. All PVC rounded fittings were drilled and tapered and 0.5-inch brass nozzles were installed. The packing of each column was done in multiple stages. For the eight big columns, the first three layers from the bottom were gravel only. Starting with two layers of gravel 200 g each, then a third 100 g layer. A tampering rod was used to pack each layer three times and the whole column was placed on a shaker for 10 seconds after every layer. The height of the three layers of gravel differed from column to column due to random particle shape but was maintained in a range between 15 to 18 cm. The packing of the sand was done similarly, in increments of 200 g. Each of the columns took around eight to nine layers of sand,



before topping off until full for a total weight ranging between 1450 and 1800 g, and a total height ranging between 44 to 47 cm. The packing of the three smaller columns was done with the same procedure but with smaller increments of 100 g in two layers then topped off for a total weight of material around 225 g.



Figure 4.2: Representation of the dimensions and layers heights of the columns used in the water quality test.

#### 4.2.2. Turbidity Stress Test Setup

The operation of the turbidity test was similar to the water quality test. A 5-gal bucket was used as the influent reservoir. Due to the settlement of particles a steel rod was used to stir the influent. A single line of Masterflex L/S 14 tubing with an inner diameter of 1.6 mm was passed from the reservoir through a Masterflex Easy-Load II pump head (connected to a Cole-Parmer 7553-70 Pump) into the column. Two columns were tested during the turbidity stress test, one containing the GCOS as the filtration media and the other containing the ROS as the filtration media. The columns used were *Drierite* indicating gas drying units repurposed for this experiment. The influent line ran from the top of the column and the bottom nozzle was used for the outflow. The inlet top nozzle was kept for the overflow – if clogging was occurring. Both GCOS and ROS were packed similarly. A coarse mesh was used to keep the content of the column elevated, then a layer of gravel 100 g in weight and around 35 mm in thickness followed by a fine mesh. Another layer of 50 g of gravel (15 mm thickness) was added topped with another fine mesh. 570 g of sand was packed into the columns topped with a coarse mesh that acted as a diffuser of the flow (Figure 4.3). The outflow was collected in a beaker to keep track of the outflow.

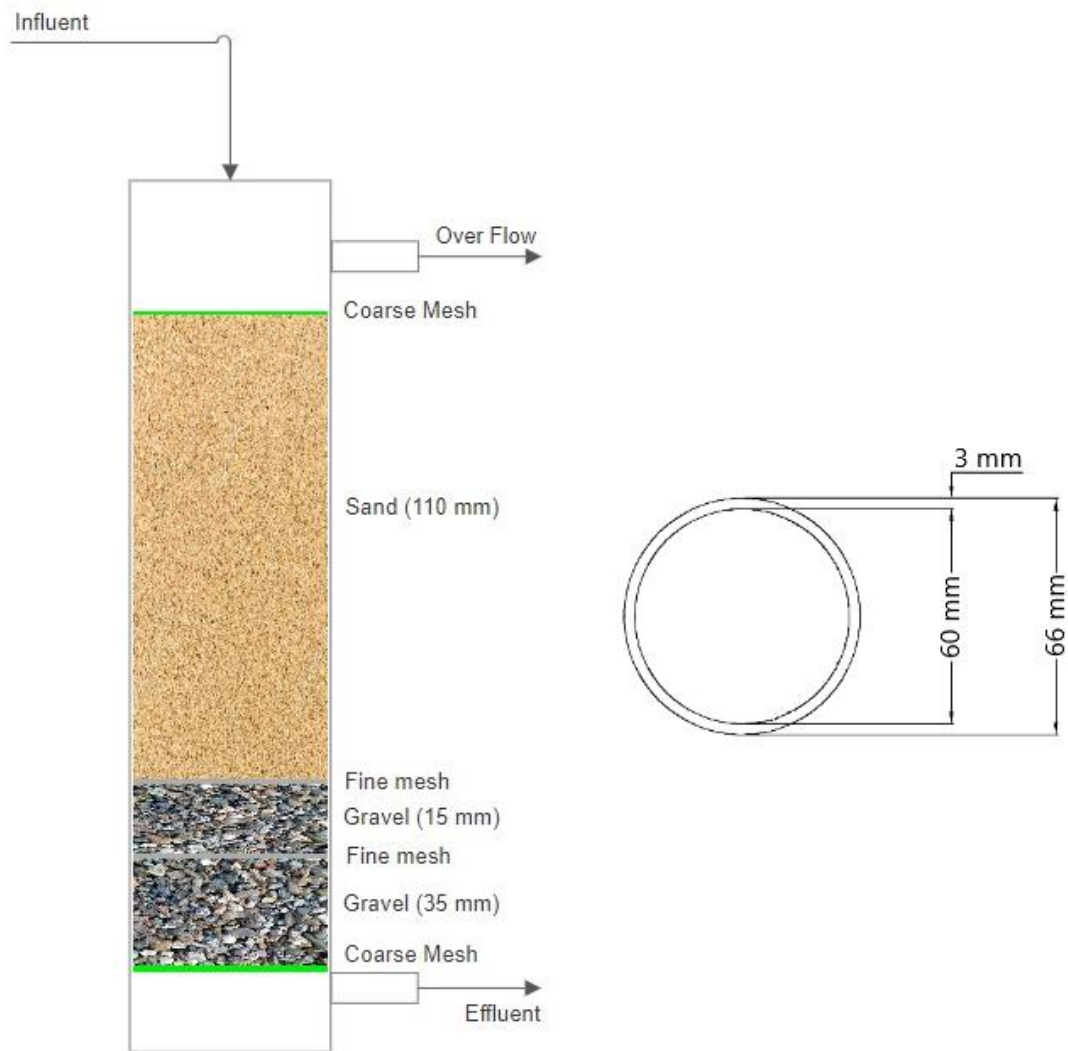


Figure 4.3: Representation of the dimensions and layers heights of the columns used in the turbidity stress test.

## 4.3. Analytical methods

### 4.3.1. Turbidity

Turbidity was measured using a wireless turbidity sensor (PASCO Scientific). The probe was calibrated daily at the beginning of each analysis using a two-point calibration (0 and

100 NTU). The values of the influent and effluent turbidity were measured every 15 min for 6 hr for a total of 24 data points. Quality assurance and quality control samples (e.g., laboratory blanks, laboratory fortified blanks, and duplicated samples) were implemented.

#### 4.3.2. Electrical Conductivity (EC)

EC was measured using a wireless EC sensor (PASCO Scientific). The probe was calibrated daily at the beginning of each analysis using a single-point blank calibration (0  $\mu\text{S}/\text{cm}$ ). Quality assurance and quality control samples (e.g., laboratory blanks, laboratory fortified blanks, and duplicated samples) were implemented.

#### 4.3.3. Total coliforms and *E. coli*

Total coliform and *E. coli* were quantified using a commercial Most Probable Number (MPN) test, Colilert 18, with a Quanti-Tray 2000 from IDEXX Laboratories (Westbrook, ME, USA) (ISO, 2012; U.S. EPA, 2005). Samples were collected aseptically and immediately after the collection, 100 ml or an appropriate dilution of the sample was mixed with the reagent, poured into sterile trays, heat-sealed, and incubated at 35 °C for 24 h to detect total coliform and *E. coli*. Bacterial removal was always determined by comparing the number of total coliforms and *E. coli* in the influent (feed water) against the numbers in the effluent from the SSF or from the two sampling ports.

## 4.4. Results and discussions

### 4.4.1. Total Coliform and *E. coli* Removal

Total coliform describes several *Enterobacteriaceae* including *E. coli* (Sahota et al., 2010). According to the EPA, the presence of coliform and *E. coli* is an indicator of fecal contamination in the water from human or animal wastes (US EPA, 2015). Although not a threat by themselves, their presence indicates whether other potentially harmful pathogens may be present in the same sample (US EPA, 2015). The regulations in terms of total coliforms and *E. coli* limit it to no more than 5% of the samples collected can be coliform positive in a month (1 sample if the total number of samples is less than 40 per month) (US EPA, 2015). For this test the total coliform in the selected water source was low. Hence, the test was carried out after rainy days. The number of total coliforms increases after precipitation due to runoff from range lands, stormwater overflow, and sewage discharges from WWTPs (Hill et al., 2006). The first sample was collected from Patsy lake on Thursday, November 23<sup>rd</sup>, 2021 after a 4 hr rain event. The initial total coliform and *E. coli* of the influent was 2987 MPN/100 ml and 238 MPN/100 ml (Figure 4.4).

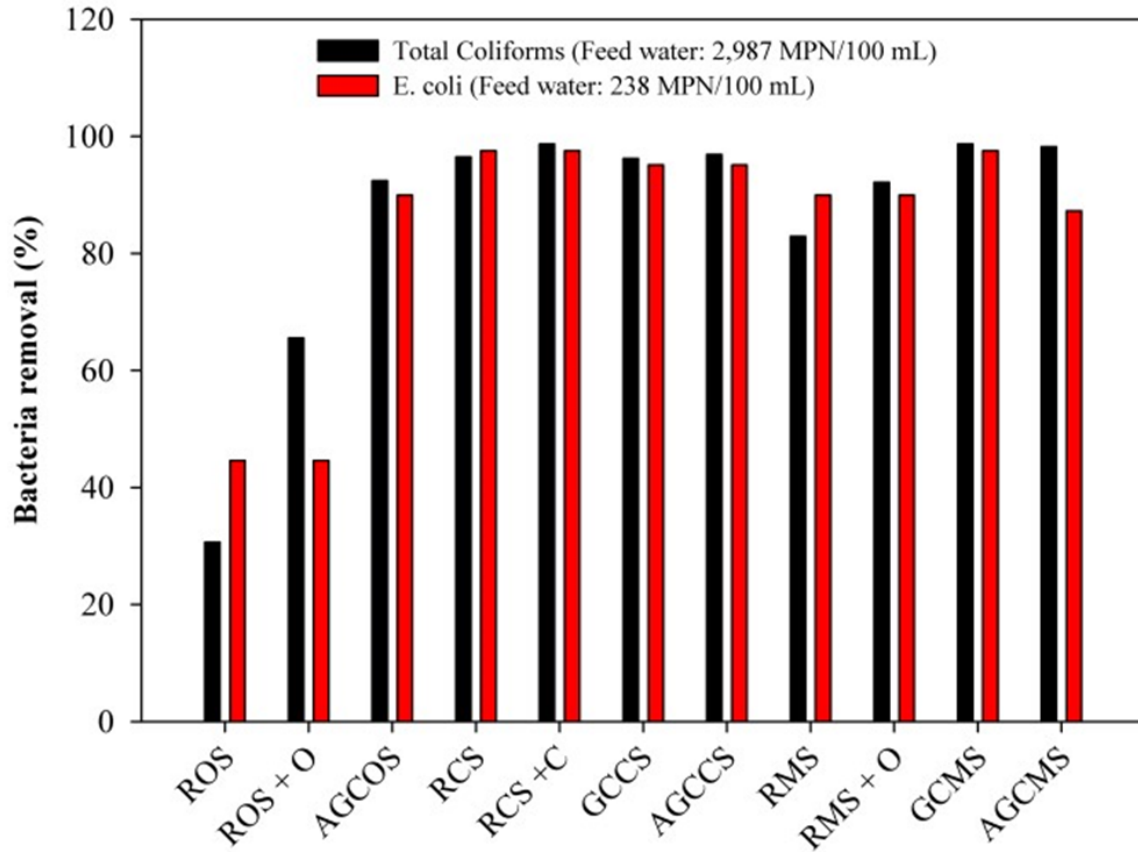


Figure 4.4: Total Bacteria Removal for ROS, RCS, RMS, GCCS, GCMS, AGCOS, AGCCS, AGCMS, O, C, and M. [ROS: raw Ottawa sand., GCCS: raw concrete sand; GCMS: raw masonry sand; GCOS: graphene coated Ottawa sand, GCCS: graphene coated concrete sand; GCMS: graphene coated masonry sand; AGCOS: activated graphene coated Ottawa sand, AGCCS: activated graphene coated concrete sand; AGCMS: activated graphene coated masonry sand.

The removal capability was increased in both the Ottawa and masonry sand when coated with graphene. The removal efficient was maintained at high levels (above 90%) in the concrete sand after coating. The activation does not seem to add any improvement to the performance of the graphene coated sand.

#### 4.4.2. Turbidity Stress Test

The turbidity stress test was run twice with two different filtration media. The conditions were maintained as identical as possible between both runs. For the first run using GCOS as the filtration media, the initially spiked turbidity of the influent was 92 NTU. In the second run with ROS, the filtration media was fed with water with an initial turbidity of was 97 NTU. The artificial initial turbidity was created by weighting 100 g of dirt in a 1000 ml beaker, adding water, and dumping the suspended particles only into the reservoir. The 1000 ml beaker was filled up and skimmed twice, then 18 L of tap water was added to the reservoir to get a dilution on 1:10. This method was accurate in acquiring similar initial turbidity. The influent was kept undisturbed during the first 150 min of the test. During the rest of the test, the influent was spiked with the maximum possible value one scope of the same dirt could acquire, which was around 500 NTU. A metal rod was used to mix the influent water to maintain the turbidity and stop the effect of particle settling. The intensity of the stirring was done relative to the running average of the influent turbidity to maintain similar influent turbidity between both tests. It is also worth mentioning that the average turbidity for the influent of the GCOS was 7 NTU higher than the average influent turbidity of the ROS.

As anticipated for both runs the removal percentage decreased with time for both runs, though the initial removal was less in the ROS and the decrease in efficiency was more noticeable over time, as shown in figure 4.5. GCOS maintained removal efficiency higher than 40% until the 345-minute mark. Meanwhile, ROS dropped under 40% after 210 minutes. Additionally, GCOS kept removing the turbidity till the end of the test in values higher than 25%. While ROS failed at minute 315, where the effluent turbidity was higher than the influent

turbidity. Upon further inspection of the columns, the fine particle build-up was spread throughout the GCOS with more built-up near the top layer. As for the ROS, the fine particle build-up was concentrated at the upper and lower fine meshes and the failure occurred after the lower fine mesh gave out and could not hold any more fine particles (figure 4.6.). The effluent out flowing rate was measured with every turbidity measurement to keep track of any changes in the flow to spot clogging, the overall change in flow rate in both runs was less than 2%. Therefore, no clogging was registered.

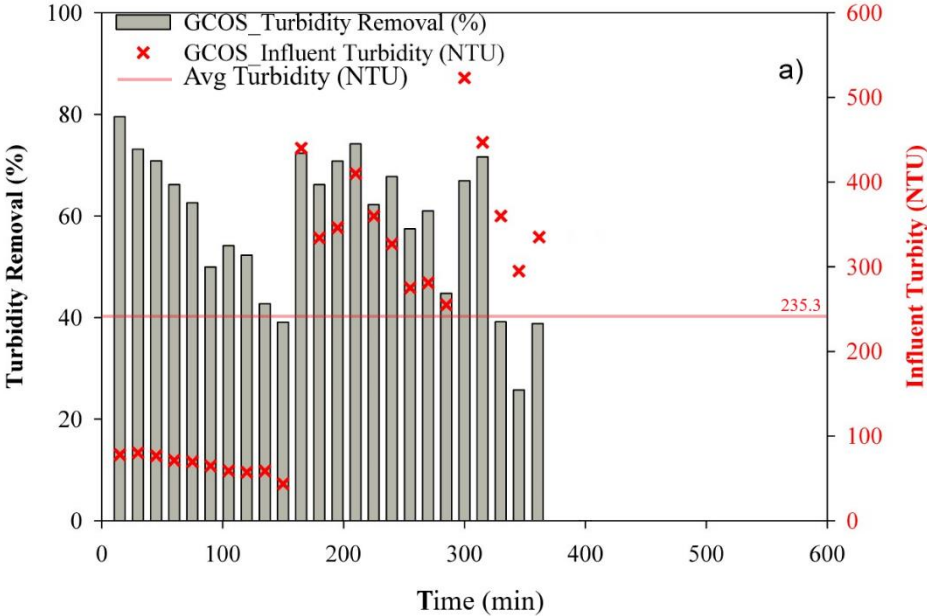


Figure 4.5: Turbidity removal and influent turbidity during the turbidity stress test for GCOS. [GCOS: Graphene coated Ottawa sand].



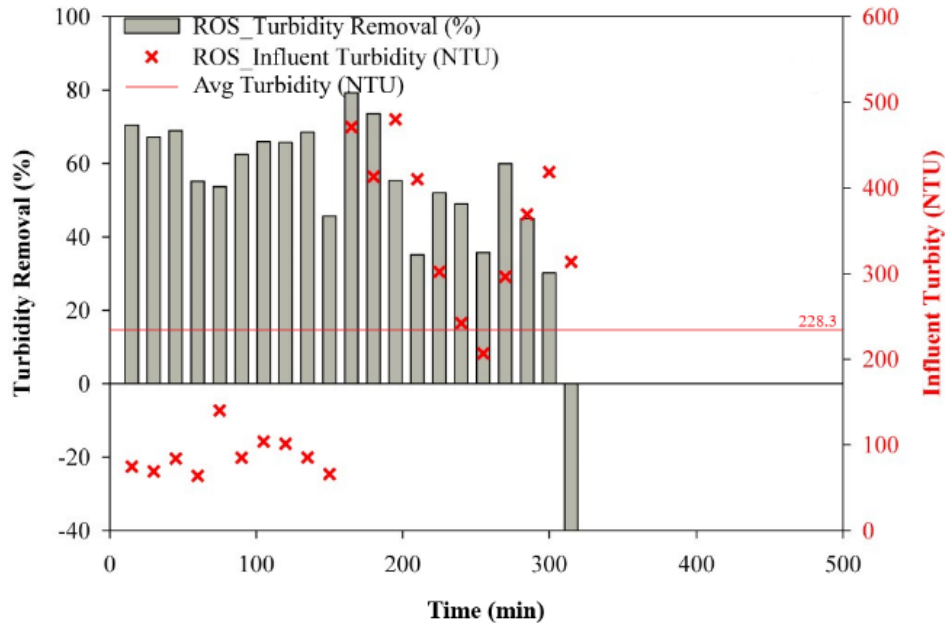


Figure 4.6: Turbidity removal and influent turbidity during the turbidity stress test for ROS. [ROS: raw Ottawa sand].

#### 4.3.3. EC:

The EC measurement of the influent was low, meaning the lake water already had a low level of dissolved substances. The EC was monitored continuously for the first two weeks for the water quality test setup (Figure 4.7). All eleven columns had similarly high values in the first 24 hr of the test. This output of dissolved substances is normal in the washing stage of any filter. Masonry sand in all its iterations had the highest initial value except in its raw form. Ottawa sand had the highest value as a raw sand filter. After the seventh day, all EC values plateaued to lower values between 40 and 50  $\mu\text{S}/\text{cm}$ .

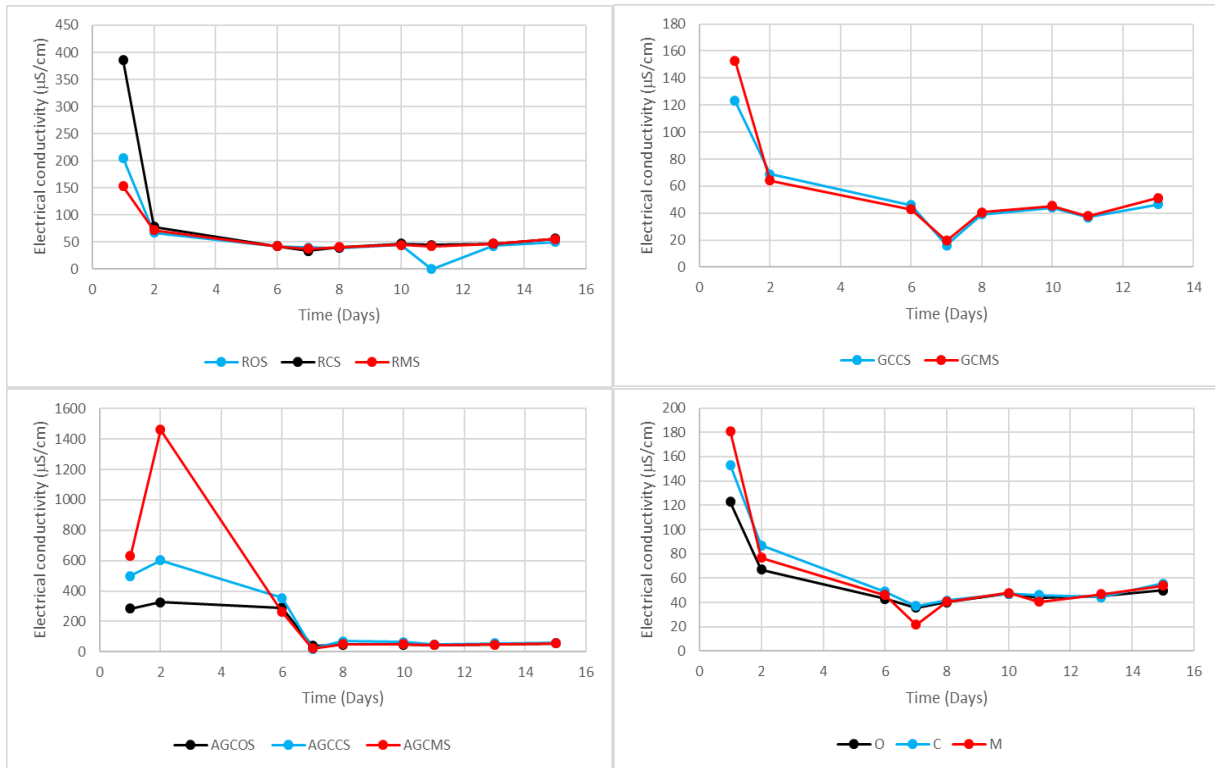


Figure 4.7: electrical conductivity for ROS, RCS, RMS, GCCS, GCMS, AGCOS, AGCCS, AGCMS, O, C, and M. [ROS: raw Ottawa sand., GCCS: raw concrete sand; GCMS: raw masonry sand; GCOS: graphene coated Ottawa sand, GCCS: graphene coated concrete sand; GCMS: graphene coated masonry sand; AGCOS: activated graphene coated Ottawa sand, AGCCS: activated graphene coated concrete sand; AGCMS: activated graphene coated masonry sand]

## CHAPTER 5. CONCLUSIONS:

The method of dehydrogenation of sugar-coated sand into a carbon-based material is a valid method of synthesizing graphene. The graphene coated sand has improved the overall results of the water filtration effectiveness.

The characteristics of the material used as the nuclei effects directly the efficiency of the graphene coating. Particle shape has the largest effect on the coating efficiency, subangular particles have a coating efficiency 30% higher than rounded particles. However, the type of the material has a smaller effect, rock fragments tend to still be coated as well as pure silica particles.

The effect of the particle shape changed the quantity of the graphene but not the quality. The Raman spectroscopy showed higher peak intensity for GCCS and GCMS by 30% compared to GCOS. The quantification was done using the EDS for the true value of carbon content by weight percentage which was found to be 71%, 64%, and 56% for GCCS, GCMS, and GCOS respectively.

The activation of the graphene coated sand had a very small effect on the apparent characteristics of the material. The activation resulted in developing cracks on the surface of the graphene making the particles' surface area larger. On the other hand, the loss of some of the graphene coating was noticed. The EDS for activated carbons results were 69%, 55%, and 50% for AGCCS, AGCMS, and AGCOS respectively.

The graphene coated material outperforms the raw material in turbidity removal. GCOS turbidity removal was 10% higher than ROS. Additionally, ROS withstood the turbidity stress

test for 300 min before failing, while GCOS continued 360 min with reduced efficiency but no signs of failing.

Electrical conductivity test showed that graphene-coated and activated graphene-coated sands tend to deposit more dissolved substances during only the first 24 hr of testing compared to raw sand filters.

Bacteria test showed that for sands with lower efficiency in removal of total coliforms and *E. coli* were further improved after coating with graphene. But the activation of the graphene coating did not further improve its effectiveness in bacteria removal and the increased cost cannot be justified at this point. A complete study of other parameters needs to be done before a final decision is made about the coating feasibility.

## FUTURE RESEARCH:

1. Further testing needs to be done on other water quality parameters of all the columns for longer period of time. Parameters such as: DOC removal, NO<sub>x</sub> removal, and metal removal.
2. Running a cost analysis that includes both the activated and non-activated graphene sand to further estimate the feasibility of the activation process vs. benefits.
3. Using molecular dynamic simulation to study the graphene coated material and the possibility of adding functional groups to enhance the removal of specific pharmaceutical contaminants.
4. Using and testing the addition of nano-additives like nano-silver before the graphitization process for further improvement to the graphene coated sands.

## Bibliography

- Adin, A. (2003). Slow granular filtration for water reuse. *Water Supply*, 3(4), 123–130.  
<https://doi.org/10.2166/ws.2003.0053>
- Álvarez-Torrellas, S., Rodríguez, A., Ovejero, G., & García, J. (2016). Comparative adsorption performance of ibuprofen and tetracycline from aqueous solution by carbonaceous materials. *Chemical Engineering Journal*, 283, 936–947.  
<https://doi.org/10.1016/j.cej.2015.08.023>
- Andreadakis, A. D., & Christoulas, D. G. (1982). On site filtration and subsurface disposal of domestic sewage. *Environmental Technology Letters*, 3(1-11), 69–74.  
<https://doi.org/10.1080/09593338209384100>
- Antunes, S. C., Freitas, R., Figueira, E., Gonçalves, F., & Nunes, B. (2013). Biochemical effects of acetaminophen in aquatic species: edible clams *Venerupis decussata* and *Venerupis philippinarum*. *Environmental Science and Pollution Research*, 20(9), 6658–6666. <https://doi.org/10.1007/s11356-013-1784-9>
- Aslan, S., & Cakici, H. (2007). Biological denitrification of drinking water in a slow sand filter. *Journal of Hazardous Materials*, 148(1-2), 253–258.  
<https://doi.org/10.1016/j.jhazmat.2007.02.012>
- Barreto, A., Luis, L. G., Soares, A. M. V. M., Paíga, P., Santos, L. H. M. L. M., Delerue-Matos, C., Hylland, K., Loureiro, S., & Oliveira, M. (2017). Genotoxicity of gemfibrozil in the gilthead seabream ( *Sparus aurata* ). *Mutation Research/Genetic Toxicology and Environmental Mutagenesis*, 821, 36–42.  
<https://doi.org/10.1016/j.mrgentox.2017.05.011>

- Bourne, D. G., Blakeley, R. L., Riddles, P., & Jones, G. J. (2006). Biodegradation of the cyanobacterial toxin microcystin LR in natural water and biologically active slow sand filters. *Water Research*, *40*(6), 1294–1302.  
<https://doi.org/10.1016/j.watres.2006.01.022>
- Campos, L. C., Su, M. F. J., Graham, N. J. D., & Smith, S. R. (2002). Biomass development in slow sand filters. *Water Research*, *36*(18), 4543–4551.  
[https://doi.org/10.1016/s0043-1354\(02\)00167-7](https://doi.org/10.1016/s0043-1354(02)00167-7)
- Chamara, P. L., & Koichi, Y. (2017). Impact of Population Growth on the Water Quality of Natural Water Bodies. *Sustainability*, *9*(8), 1405. <https://doi.org/10.3390/su9081405>
- Dafouz, R., Cáceres, N., Rodríguez-Gil, J. L., Mastroianni, N., López de Alda, M., Barceló, D., de Miguel, Á. G., & Valcárcel, Y. (2018). Does the presence of caffeine in the marine environment represent an environmental risk? A regional and global study. *Science of the Total Environment*, *615*, 632–642.  
<https://doi.org/10.1016/j.scitotenv.2017.09.155>
- De Gisi, S., Lofrano, G., Grassi, M., & Notarnicola, M. (2016). Characteristics and adsorption capacities of low-cost sorbents for wastewater treatment: A review. *Sustainable Materials and Technologies*, *9*, 10–40. <https://doi.org/10.1016/j.susmat.2016.06.002>
- Dev, A., Dilly, T. C., Bakhshipour, A. E., Dittmer, U., & Bhallamudi, S. M. (2021). Optimal Implementation of Wastewater Reuse in Existing Sewerage Systems to Improve Resilience and Sustainability in Water Supply Systems. *Water*, *13*(15), 2004.  
<https://doi.org/10.3390/w13152004>
- Dubey, R., Bajpai, J., & Bajpai, A. K. (2015). Green synthesis of graphene sand composite (GSC) as novel adsorbent for efficient removal of Cr (VI) ions from aqueous solution.



*Journal of Water Process Engineering*, 5, 83–94.

<https://doi.org/10.1016/j.jwpe.2015.01.004>

Elbana, M., Ramírez de Cartagena, F., & Puig-Bargués, J. (2012). Effectiveness of sand media filters for removing turbidity and recovering dissolved oxygen from a reclaimed effluent used for micro-irrigation. *Agricultural Water Management*, 111, 27–33.

<https://doi.org/10.1016/j.agwat.2012.04.010>

Ewen Smith, & Dent, G. (2019). *Modern Raman spectroscopy : a practical approach*. Hoboken, Nj Wiley.

Fan, D., Lue, L., & Yang, S. (2017). Molecular dynamics study of interfacial stress transfer in graphene-oxide cementitious composites. *Computational Materials Science*, 139, 56–64. <https://doi.org/10.1016/j.commatsci.2017.07.034>

Geim, A. K., & Novoselov, K. S. (2007). The rise of graphene. *Nature Materials*, 6(3), 183–191. <https://doi.org/10.1038/nmat1849>

Gupta, S. S., Sreepasad, T. S., Maliyekkal, S. M., Das, S. K., & Pradeep, T. (2012). Graphene from Sugar and its Application in Water Purification. *ACS Applied Materials & Interfaces*, 4(8), 4156–4163. <https://doi.org/10.1021/am300889u>

Hijosa-Valsero, M., Matamoros, V., Sidrach-Cardona, R., Pedescoll, A., Martín-Villacorta, J., García, J., Bayona, J. M., & Bécares, E. (2011). Influence of design, physico-chemical and environmental parameters on pharmaceuticals and fragrances removal by constructed wetlands. *Water Science and Technology*, 63(11), 2527–2534.

<https://doi.org/10.2166/wst.2011.500>

Hill, D., Owens, W., & Tchounwou, P. (2006). The Impact of Rainfall on Fecal Coliform Bacteria in Bayou Dorcheat (North Louisiana). *International Journal of*

*Environmental Research and Public Health*, 3(1), 114–117.

<https://doi.org/10.3390/ijerph2006030013>

Ives, KJ. (1980). *Filtration & separation*. Uplands Press.

Katukiza, A. Y., Ronteltap, M., Niwagaba, C. B., Kansime, F., & Lens, P. N. L. (2014). Grey water treatment in urban slums by a filtration system: Optimisation of the filtration medium. *Journal of Environmental Management*, 146, 131–141.

<https://doi.org/10.1016/j.jenvman.2014.07.033>

Kim, K.-H., Kabir, E., & Jahan, S. A. (2017). Exposure to pesticides and the associated human health effects. *Science of the Total Environment*, 575, 525–535.

<https://doi.org/10.1016/j.scitotenv.2016.09.009>

Kimbrough, K. L., & Center For Coastal Monitoring And Assessment (U.S. (2008). *An assessment of two decades of contaminant monitoring in the nation's coastal zone*.

National Oceanic And Atmospheric Administration, National Ocean Service, National Centers For Coastal Ocean Science, Center For Coastal Monitoring And Assessment.

Köck-Schulmeyer, M., Villagrasa, M., López de Alda, M., Céspedes-Sánchez, R., Ventura, F., & Barceló, D. (2013). Occurrence and behavior of pesticides in wastewater treatment plants and their environmental impact. *Science of the Total Environment*, 458-460, 466–476.

<https://doi.org/10.1016/j.scitotenv.2013.04.010>

Kolar, B., Arnuš, L., Jeretin, B., Gutmaher, A., Drobne, D., & Durjava, M. K. (2014). The toxic effect of oxytetracycline and trimethoprim in the aquatic environment.

*Chemosphere*, 115, 75–80. <https://doi.org/10.1016/j.chemosphere.2014.02.049>

Kookana, R. S., Ying, G-G., & Waller, N. J. (2011). Triclosan: its occurrence, fate and effects in the Australian environment. *Water Science and Technology*, 63(4), 598–604.

<https://doi.org/10.2166/wst.2011.205>

Kumar, P., Rehab, H., Hegde, K., Brar, S. K., Cledon, M., Kermanshahi-pour, A., Vo Duy, S., Sauvé, S., & Surampalli, R. Y. (2020). Physical and biological removal of Microcystin-LR and other water contaminants in a biofilter using Manganese Dioxide coated sand and Graphene sand composites. *Science of the Total Environment*, 703, 135052. <https://doi.org/10.1016/j.scitotenv.2019.135052>

L Huisman, & Wood, W. E. (1974). *Slow sand filtration*. Geneva: World Health Organization.

Larkin, P. (2011). *Infrared and raman spectroscopy : principles and spectral interpretation*. Elsevier, Cop.

Leite, A. J. B., A., C. S., Thue, P. S., dos Reis, G. S., Dias, S. L. P., Lima, E. C., Vaghetti, J. C. P., Pavan, F. A., & de Alencar, W. S. (2017). Activated carbon from avocado seeds for the removal of phenolic compounds from aqueous solutions. *DESALINATION and WATER TREATMENT*, 71, 168–181. <https://doi.org/10.5004/dwt.2017.20540>

Lofrano, G., & Brown, J. (2010). Wastewater management through the ages: A history of mankind. *Science of the Total Environment*, 408(22), 5254–5264. <https://doi.org/10.1016/j.scitotenv.2010.07.062>

Mackenzie Leo Davis. (2020). *Water and wastewater engineering : design principles and practice*. Mcgraw-Hill.

Mangalgi, K. P., He, K., & Blaney, L. (2015). Emerging Contaminants: A Potential Human Health Concern for Sensitive Populations. *PDA Journal of Pharmaceutical Science and Technology*, 69(2), 215–218. <https://doi.org/10.5731/pdajpst.2015.01034>

Marques, S. C. R., Marcuzzo, J. M., Baldan, M. R., Mestre, A. S., & Carvalho, A. P. (2017). Pharmaceuticals removal by activated carbons: Role of morphology on cyclic thermal

regeneration. *Chemical Engineering Journal*, 321, 233–244.

<https://doi.org/10.1016/j.cej.2017.03.101>

Matamoros, V., Arias, C., Brix, H., & Bayona, J. M. (2009). Preliminary screening of small-scale domestic wastewater treatment systems for removal of pharmaceutical and personal care products. *Water Research*, 43(1), 55–62.

<https://doi.org/10.1016/j.watres.2008.10.005>

Mays, L. W. (2013). A brief history of water filtration/sedimentation. *Water Science and Technology: Water Supply*, 13(3), 735–742. <https://doi.org/10.2166/ws.2013.102>

Mcmullan, D. (2006). Scanning electron microscopy 1928-1965. *Scanning*, 17(3), 175–185.

<https://doi.org/10.1002/sca.4950170309>

Moradi, S., & Azizian, S. (2016). Preparation of nanostructured carbon covered sand for removal of methyl violet from water. *Journal of Molecular Liquids*, 219, 909–913.

<https://doi.org/10.1016/j.molliq.2016.03.075>

Nakhla, G., & Farooq, S. (2003). Simultaneous nitrification–denitrification in slow sand filters. *Journal of Hazardous Materials*, 96(2-3), 291–303.

[https://doi.org/10.1016/s0304-3894\(02\)00219-4](https://doi.org/10.1016/s0304-3894(02)00219-4)

Nawaz, T., & Sengupta, S. (2019). Contaminants of Emerging Concern: Occurrence, Fate, and Remediation. *Advances in Water Purification Techniques*, 67–114.

<https://doi.org/10.1016/b978-0-12-814790-0.00004-1>

Qu, H., Barrett, H., Wang, B., Han, J., Wang, F., Gong, W., Wu, J., Wang, W., & Yu, G. (2021). Co-occurrence of antiseptic triclocarban and chiral anti-inflammatory ibuprofen in environment: Association between biological effect in sediment and risk to human health. *Journal of Hazardous Materials*, 407, 124871.

<https://doi.org/10.1016/j.jhazmat.2020.124871>

- Raman, C. V., & Krishnan, K. S. (1928). A New Type of Secondary Radiation. *Nature*, *121*(3048), 501–502. <https://doi.org/10.1038/121501c0>
- Rodgers, M., Mulqueen, J., & Healy, M. G. (2004). Surface Clogging in an Intermittent Stratified Sand Filter. *Soil Science Society of America Journal*, *68*(6), 1827–1832. <https://doi.org/10.2136/sssaj2004.1827>
- Rostvall, A., Zhang, W., Dürig, W., Renman, G., Wiberg, K., Ahrens, L., & Gago-Ferrero, P. (2018). Removal of pharmaceuticals, perfluoroalkyl substances and other micropollutants from wastewater using lignite, Xylit, sand, granular activated carbon (GAC) and GAC+Polonite® in column tests – Role of physicochemical properties. *Water Research*, *137*, 97–106. <https://doi.org/10.1016/j.watres.2018.03.008>
- Sahota, P., Pandove, G., Achal, V., & Vikal, Y. (2010). Evaluation of a BWTK for detection of total coliforms, E. Coli and emerging pathogens from drinking water: comparison with standard MPN method. *Water Science and Technology*, *62*(3), 676–683. <https://doi.org/10.2166/wst.2010.330>
- Sirés, I., & Brillas, E. (2012). Remediation of water pollution caused by pharmaceutical residues based on electrochemical separation and degradation technologies: A review. *Environment International*, *40*, 212–229. <https://doi.org/10.1016/j.envint.2011.07.012>
- Slavik, I., Jehmlich, A., & Uhl, W. (2013). Impact of backwashing procedures on deep bed filtration productivity in drinking water treatment. *Water Research*, *47*(16), 6348–6357. <https://doi.org/10.1016/j.watres.2013.08.009>
- Sophia A., C., & Lima, E. C. (2018). Removal of emerging contaminants from the environment by adsorption. *Ecotoxicology and Environmental Safety*, *150*, 1–17.

<https://doi.org/10.1016/j.ecoenv.2017.12.026>

Sundaresan, B. B., & Paramasivam, R. (1982). *Slow Sand Filtration Research and Demonstration Project- India. NEERI, Nagpur, India.*

Tchobanoglous, G., Burton, F. L., H David Stensel, & Inc, E. (2004). *废水工程：处理及回用 = Wastewater engineering : treatment and reuse / Fei shui gong cheng : chu li ji hui yong = Wastewater engineering : treatment and reuse.* Hua Xue Gong Ye Chu Ban She.

Torrellas, S. Á., García Lovera, R., Escalona, N., Sepúlveda, C., Sotelo, J. L., & García, J. (2015). Chemical-activated carbons from peach stones for the adsorption of emerging contaminants in aqueous solutions. *Chemical Engineering Journal*, 279, 788–798.  
<https://doi.org/10.1016/j.cej.2015.05.104>

Tyagi, V. K., Khan, A. A., Kazmi, A. A., Mehrotra, I., & Chopra, A. K. (2009). Slow sand filtration of UASB reactor effluent: A promising post treatment technique. *Desalination*, 249(2), 571–576. <https://doi.org/10.1016/j.desal.2008.12.049>

UNESCO. (2015). *Water for a sustainable world.* United Nations Educational, Scientific And Cultural Organization.

UNESCO. (2017). *Wastewater : the untapped resource : the United Nations world water development report 2017.* United Nations Education, Scientific And Cultural Organization.

UNESCO. (2003). ICID related sessions at 3rd World Water Forum in Kyoto, Japan. *Irrigation and Drainage*, 52(2), 191–192. <https://doi.org/10.1002/ird.84>

US EPA. (2015a, September 3). *Drinking Water Regulations and Contaminants.* US EPA.  
<https://www.epa.gov/sdwa/drinking-water-regulations-and-contaminants>

- US EPA. (2014, May 6). *Contaminant Candidate List 4-CCL 4*. Wwww.epa.gov.  
<https://www.epa.gov/ccl/contaminant-candidate-list-4-ccl-4-0>
- US EPA. (2015b, November 30). *National Primary Drinking Water Regulations*.  
Wwww.epa.gov. <https://www.epa.gov/ground-water-and-drinking-water/national-primary-drinking-water-regulations#five>
- Verma, S., Daverey, A., & Sharma, A. (2017). Slow sand filtration for water and wastewater treatment – a review. *Environmental Technology Reviews*, 6(1), 47–58.  
<https://doi.org/10.1080/21622515.2016.1278278>
- Viegas, R. M. C., Mestre, A. S., Mesquita, E., Campinas, M., Andrade, M. A., Carvalho, A. P., & Rosa, M. J. (2020). Assessing the applicability of a new carob waste-derived powdered activated carbon to control pharmaceutical compounds in wastewater treatment. *Science of the Total Environment*, 743, 140791.  
<https://doi.org/10.1016/j.scitotenv.2020.140791>
- Vigil, P., del Río, J. P., Carrera, B., Aránguiz, F. C., Rioseco, H., & Cortés, M. E. (2016). Influence of Sex Steroid Hormones on the Adolescent Brain and Behavior: An Update. *The Linacre Quarterly*, 83(3), 308–329.  
<https://doi.org/10.1080/00243639.2016.1211863>
- Visscher, J. T. (1990). Slow Sand Filtration: Design, Operation, and Maintenance. *Journal - American Water Works Association*, 82(6), 67–71. <https://doi.org/10.1002/j.1551-8833.1990.tb06979.x>
- Wakelin, S. A., Colloff, M. J., & Kookana, R. S. (2008). Effect of Wastewater Treatment Plant Effluent on Microbial Function and Community Structure in the Sediment of a Freshwater Stream with Variable Seasonal Flow. *Applied and Environmental*

*Microbiology*, 74(9), 2659–2668. <https://doi.org/10.1128/aem.02348-07>

Wang, J., Da, L., Song, K., & Li, B.-L. (2008). Temporal variations of surface water quality in urban, suburban and rural areas during rapid urbanization in Shanghai, China.

*Environmental Pollution*, 152(2), 387–393.

<https://doi.org/10.1016/j.envpol.2007.06.050>

Watt, I. M. (1978). A comparison of gold and platinum sputtered coatings for scanning electron microscopy. *Proceedings, Annual Meeting, Electron Microscopy Society of America*, 36(2), 94–95. <https://doi.org/10.1017/s0424820100081334>

Weigel, S., Berger, U., Jensen, E., Kallenborn, R., Thoresen, H., & Hühnerfuss, H. (2004). Determination of selected pharmaceuticals and caffeine in sewage and seawater from Tromsø/Norway with emphasis on ibuprofen and its metabolites. *Chemosphere*, 56(6), 583–592. <https://doi.org/10.1016/j.chemosphere.2004.04.015>

Wojcieszynska, D., & Guzik, U. (2020). Naproxen in the environment: its occurrence, toxicity to nontarget organisms and biodegradation. *Applied Microbiology and Biotechnology*, 104(5), 1849–1857. <https://doi.org/10.1007/s00253-019-10343-x>

Young-Rojanschi, C., & Madramootoo, C. (2014). Intermittent versus continuous operation of biosand filters. *Water Research*, 49, 1–10.

<https://doi.org/10.1016/j.watres.2013.11.011>

Zheng, X., Ernst, M., & Jekel, M. (2010). Pilot-scale investigation on the removal of organic foulants in secondary effluent by slow sand filtration prior to ultrafiltration. *Water Research*, 44(10), 3203–3213. <https://doi.org/10.1016/j.watres.2010.02.038>

Zipf, M. S., Pinheiro, I. G., & Conegero, M. G. (2016). Simplified greywater treatment systems: Slow filters of sand and slate waste followed by granular activated carbon.



*Journal of Environmental Management*, 176, 119–127.

<https://doi.org/10.1016/j.jenvman.2016.03.035>

Zularisam, A. W., Wahida, N., & Alfian, A. (2017). Comparison on characteristic of Mesoparticle Graphene Sand Composite (MGSC) using different types of sugar to remove methylene blue. *IOP Conference Series: Materials Science and Engineering*, 217, 012005. <https://doi.org/10.1088/1757-899x/217/1/012005>

## Appendices



*Figure A.1: Raw sand preparation*



*Figure A.2: Sand sugar coating and graphitization.*



*Figure A.3: Water source (lake Patsy) and water collection.*



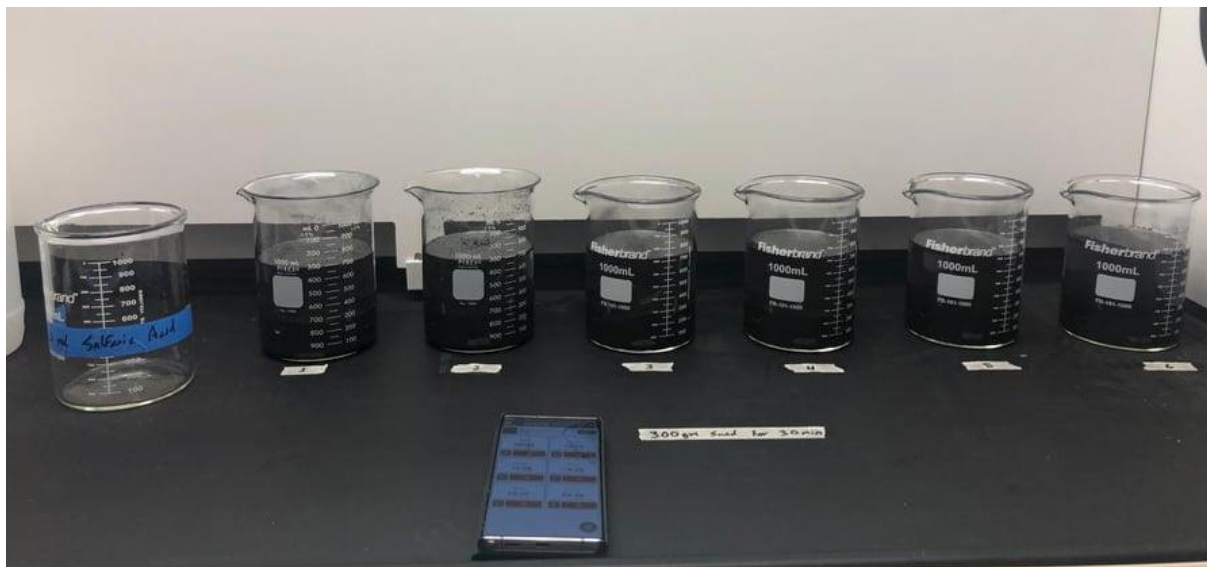


Figure A.4: Activation process using sulfuric acid.



Figure A.5: the eleven-column setup.

## VITA

**B.Sc. in Civil Engineering**, Jordan University of Science and Technology, Irbid, Jordan, 2019.